THE PROFILE OF A LIQUID DROPLET DURING FORMATION AND SEPARATION

by

James Edmund Halligan

A Dissertation Submitted to the
Graduate Faculty in Partial Fulfillment of
The Requirements for the Degree of
DOCTOR OF PHILOSOPHY

Major Subject: Chemical Engineering

Approved:

Signature was redacted for privacy.

In Charge of Major Work

Signature was redacted for privacy.

Head of Major Department

Signature was redacted for privacy.

Dean of Graduate College

Iowa State University
Of Science and Technology
Ames, Iowa

1967

TABLE OF CONTENTS

INTRODUCTION

There has been considerable interest in the shape of the profile of bubbles and droplets for over 150 years. Initially, an equation was needed to describe the shape of the meniscus and to explain the phenomenon of capillary rise. Laplace and others derived an equation which applied to a static droplet using a force balance on an element of the interface. The physical constants in this equation were the densities of the two fluids and the interfacial tension.

When the droplet was considered to be a surface of revolution, the force balance could be combined with the equations resulting from the assumption of axial symmetry to obtain a set of differential equations whose solution was the profile of the droplet. These equations could not be solved analytically but they were considered sufficiently important that they were solved by hand for a large number of cases using numerical integration. The results were used to measure the interfacial tension and are still in use today.

Because of the availability of a large, fast computer it is now possible to accomplish in a few minutes what previously required months of tedious calculation. This machine allows additional assumptions about the nature of the interface, whose validity can be determined only by the use of long and involved iteration schemes, to be investigated.

The purpose of this investigation was to determine if the equations of Laplace could be used as a basis to describe the profile of a droplet forming on a submerged plate. The effects of flow rate and orifice size on the shape of the droplet were to be studied. As a result of this, it was also

necessary to consider extending the range over which the equations were applicable by adding terms not related to flow effects.

LITERATURE REVIEW

The equations which predict the profile of a static droplet were developed by several investigators including Laplace (1). The principal expression in this development resulted from a pressure balance on a small element of the interface. Included in the balance was a term which accounted for the inward pressure due to the interfacial tension and the curvature of the surface. When the droplet was assumed to be a surface of revolution, this term permitted a set of three ordinary differential equations whose solution was the profile of the droplet to be developed.

The equations could not be solved analytically, so Bashforth and Adams (2) developed a technique to solve them numerically. In order to make their solutions as general as possible, the equations were expressed in dimensionless coordinates using a single parameter which contained all of the fluid properties. The results were published in the form of tables which contained solutions for particular values of the parameter. By considering a parameter of this type, Lohnstein (3) concluded that when the volume of the static droplet exceeded a critical value, the droplet would become unstable and a portion of it would separate from the plate.

Freud and Harkins (4) using the tables of Bashforth and Adams were able to confirm the conclusion of Lohnstein. When the parameter containing the fluid properties is plotted versus the volume of a static droplet, there is a maximum in the curve. Since the droplet may not decrease in volume, it must separate from the plate at this maximum. More importantly for this study, the equations of Laplace no longer apply once the volume exceeds the critical value. The critical volume is the maximum volume that

the droplet may contain and still be mechanically stable.

Because the equations of Laplace could not be easily manipulated mathematically, several investigators attempted to predict the volume and surface area of a forming droplet by considering the geometry of the profile (5,6) or by using dimensional analysis (7). Since the profile of a droplet may change markedly when a different plate material is used, any correlations which are based on an assumed drop geometry are necessarily very specific (8).

Attempts were also made to use the tables of Bashforth and Adams to develop correction factors which allowed simpler formulas to be used to predict the volume of a static droplet (9). These factors were then used in mathematical models which predicted the volume of the droplet at separation (10,11). The profiles of a droplet in the region where the static equation applies and those at separation are quite different and the development of a sufficiently general correction factor would be very difficult.

An excellent qualitative description of the growth of a droplet was given by Manfre' (12). This paper carefully describes the growth process and in particular, notes that the initial droplet is different from all others. Since this study was concerned with extrusion, the viscosities and orifice sizes which were considered permitted assumptions which are not reasonable for the conditions normally encountered in liquid-liquid extraction.

Several additional papers (13,14,15) have been written which illustrate how the relationship of surface area and volume to flow rate and

orifice size could be used if it were available. In many of these studies, the droplets were assumed to have a spherical geometry. An examination of the actual profiles of droplets clearly indicates how inadequate this assumption is in most cases.

DESCRIPTION OF THE PROFILE

Forming Droplet - Below Critical Volume

Any difference in the profiles of a forming and a static droplet must be a result of the motion of the fluid within the droplet. The normal path for an element of fluid to follow would be to flow directly from the orifice to the apex of the droplet and then parallel to the interface (Figure 1). The fluid element causes an outward pressure on each segment of the interface as it is diverted slightly from its path.

In order to calculate the magnitude of this pressure, several assumptions concerning the type of flow and the nature of the interface of the forming droplet are required. Plug flow with negligible viscous dissipation was assumed because the rate at which the fluid impinged upon an element of the interface could be easily calculated. The interface was assumed to have a negligible velocity relative to the fluid elements and the net force acting on any small segment of the interface was assumed to be zero. In addition, the drag due to the flow of the continuous phase on the surface of the droplet was assumed to be negligible.

For elements in plug-flow, the rate at which fluid from the orifice impinges upon a circular area, ds, located at the apex of the droplet would be $(m/\pi R^2)ds$. This impinging stream would produce a normal force, dF, on the stationary interface and would then be diverted equally in all directions in a horizontal plane tangent to the surface of the droplet (13).

$$dF = \left(\frac{m}{\pi R^2}\right)ds\left(\frac{m}{\pi DR^2}\right) \quad . \tag{1}$$

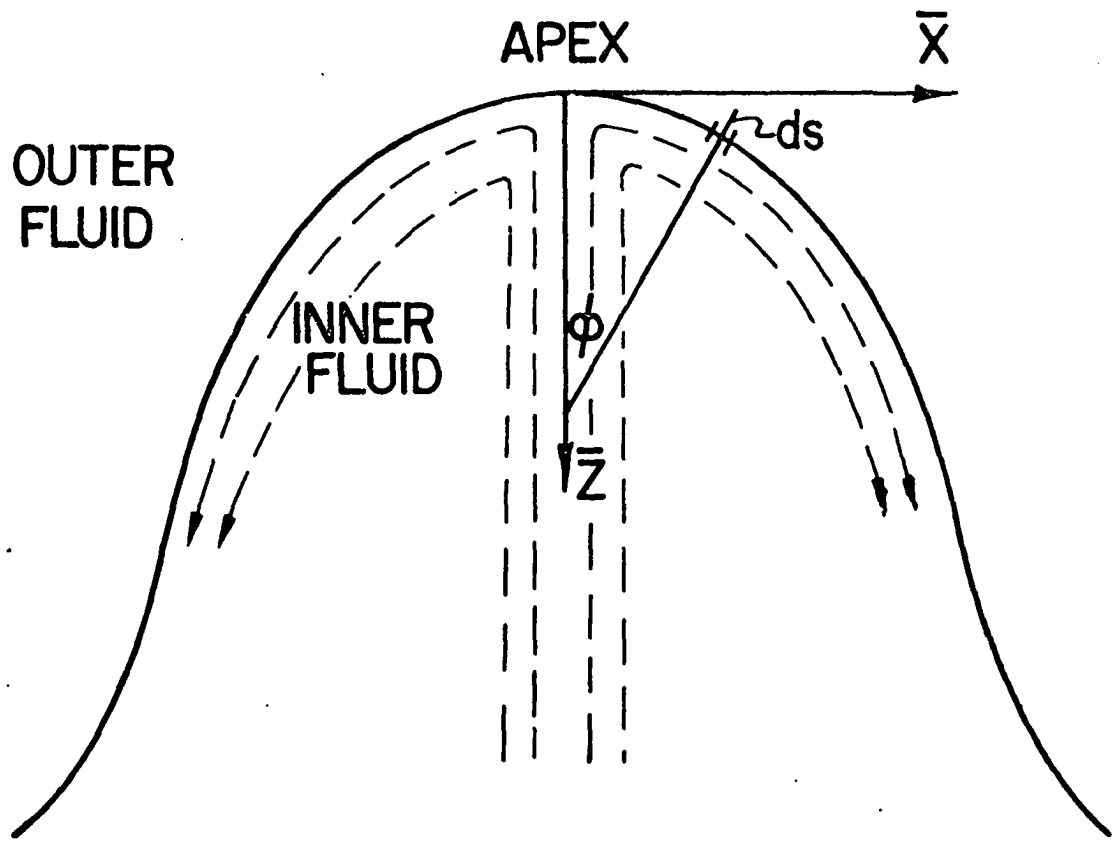

Figure 1. Diagram indicating the assumed flow pattern and coordinate system

The outward pressure at the apex of the droplet on the interface due to the movement of the fluid is then:

$$(\frac{dF}{ds})_o = (\frac{m^2}{\pi^2 R^4 D}) \quad . \tag{2}$$

This is the term which must be included in the static equations because of the motion of the fluid. Although it is valid only at the apex of the droplet and a more general term will be needed to obtain the entire profile, Equation 2 will be required when considering the pressures on a general element of surface.

Figure 2 is a force diagram for an element of surface located anywhere on the interface of the growing droplet. (dF/ds) is again the outward pressure due to the moving fluid impinging on the element. If the forces are assumed to be balanced:

$$p + T(\frac{\text{Sin}\phi}{\bar{X}} + \frac{1}{\bar{\rho}}) = P + (dF/ds) \quad . \tag{3}$$

The term $T(\frac{\text{Sin}\phi}{\bar{X}} + \frac{1}{\bar{\rho}})$, developed by Laplace and derived in the Appendix, is the pressure due to surface curvature and surface tension.

Equation 3 will now be rearranged and simplified so that it may be combined with the equations which result from the assumption of axial symmetry. The pressures P and p may be expressed in terms of their values at the origin plus a static head term.

$$P = P_o + D\, g\bar{Z} \tag{4}$$

$$p = p_o + d\, g\bar{Z} \tag{5}$$

These equations may then be combined with Equation 3.

$$p_o + dg\bar{Z} + T(\frac{\text{Sin}\phi}{\bar{X}} + \frac{1}{\bar{\rho}}) = P_o + Dg\bar{Z} + (dF/ds) \tag{6}$$

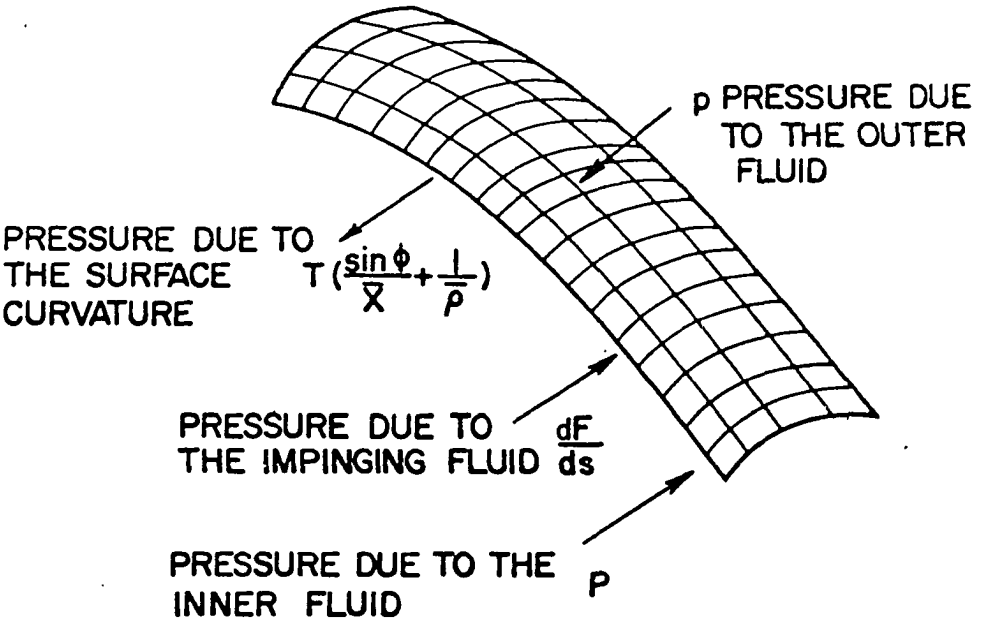

$$p + T\left(\frac{\sin\phi}{X} + \frac{1}{\rho}\right) = P + \frac{dF}{ds}$$

Figure 2. Pressure balance on an element of the interface

Using Equation 2, each of the terms may be evaluated at the origin ($\overline{X},\overline{Z} = 0$):

$$p_o + 2T/b = P_o + (m^2/\pi^2 R^4 D) \quad , \tag{7}$$

where b is the initial curvature as defined by Bashforth and Adams.

Equations 6 and 7 are then combined to eliminate the difference in pressure across the interface at the origin.

$$d g\overline{Z} + T\left(\frac{\mathrm{Sin}\phi}{\overline{X}} + \frac{1}{\overline{\rho}}\right) = \frac{2T}{b} - \frac{m^2}{\pi^2 R^4 D} + Dg\overline{Z} + \frac{dF}{ds} \quad . \tag{8}$$

This equation can be simplified by introducing dimensionless variables ($\rho = \overline{\rho}/b$, $Z = \overline{Z}/b$, $X = \overline{X}/b$) and two dimensionless groups, β and f.

$$\frac{1}{\rho} = 2.0 - f + \beta Z - \frac{\mathrm{Sin}\phi}{X} + \frac{b}{T}\left(\frac{dF}{ds}\right) \tag{9}$$

$$\beta = \frac{g(D-d)b^2}{T} \tag{10}$$

$$f = \frac{m^2 b}{\pi^2 T R^4 D} \tag{11}$$

The parameter β contains the physical properties of the fluid, while f is the dynamic pressure caused by the fluid impinging on the interface at the apex of the droplet.

Equation 9, which is in the form used in determining the profile of the growing droplet, has the same restriction as the equation of Laplace, namely that the volume of the droplet must be less than the critical value (4). As mentioned previously, the critical volume is the maximum volume which the droplet may contain and still be mechanically stable.

The additional equations necessary to obtain a solution can be

developed by considering the geometry of the interface of an axially symmetric droplet (2). These are derived in the Appendix

$$\frac{dX}{da} = \text{Cos}\phi \tag{12}$$

$$\frac{dZ}{da} = \text{Sin}\phi \tag{13}$$

$$\frac{d\phi}{da} = \frac{1}{\rho} \tag{14}$$

If the term $\frac{b}{T}\left(\frac{dF}{ds}\right)$ is adequately defined, Equations 9-14 together with the boundary conditions given in Equations 15, 16, and 17 can be solved simultaneously to determine the profile of a growing droplet.

$$\left(\frac{dX}{da}\right)_o = 1.0 \tag{15}$$

$$\left(\frac{dZ}{da}\right)_o = 0.0 \tag{16}$$

$$\left(\frac{d\phi}{da}\right)_o = 1.0 \tag{17}$$

The third boundary condition may be obtained by evaluating Equation 9 at the origin and using the relations:

$$\left(\frac{\text{Sin}\phi}{X}\right)_o = 1.0 \tag{18}$$

$$\frac{b}{T}\left(\frac{dF}{ds}\right)_o \tag{19}$$

Equation 18 is discussed in the work of Bashforth and Adams and is a result of the definition of the dimensionless coordinates.

Equation 19 indicates that the dynamic equation reduces to the static case at the apex since the dynamic terms cancel out and, therefore, the profiles of growing and static droplets should be similar near the origin. Consequently, the solution for the dynamic case may be initiated by

integrating the equations applying to the static case for a short distance along the interface.

After this initial small increment, the set of Equations 9-14 may then be integrated, provided the term $\frac{b}{T}\left(\frac{dF}{ds}\right)$, which is dependent on the rate of momentum in the stream deflected at the apex, is evaluated. Since the tangent to the surface is horizontal at the apex, the initial increment may be assumed to be flat with little error. If X_1 is the X coordinate at the end of the initial increment, the rate of momentum in the deflected stream, S_1, would be:

$$S_1 = \left(\frac{m^2 X_1^2}{\pi D R^4}\right) . \tag{20}$$

It is also necessary to know the rate of momentum in the stream of fluid coming from the orifice. The size of this stream will depend upon the amount of area the interfacial element projects in a plane parallel to the plate. If X_2 is the X coordinate at the end of the second interfacial element, the rate of momentum, S_r, in the stream coming from the orifice is:

$$S_r = \frac{m^2(X_2^2 - X_1^2)}{\pi D R^4} . \tag{21}$$

The only additional information needed before the integration can be performed for the second element are the angles at which these impinging streams strike the interfacial element. For this purpose, the average of the normal to the interface at the beginning and end of the element was used. If the total change in angle is small, the error involved should be negligible. If ϕ_2 is the average normal angle for the second

integration increment, the normal force due to the two impinging streams would be:

$$dF_2 = S_1 \, Sin\phi_2 + S_r \, Cos\phi_2 \quad . \tag{22}$$

Equation 22 applies only to the second interfacial element and a more general expression is needed for the remaining elements. This expression can be determined if it is assumed that the deflected stream leaves the interfacial element in a direction perpendicular to the average normal angle. If this is so, the rate of momentum leaving in this stream may be calculated by algebraically summing the momentum components of the two streams, S_r and S_1, in a direction parallel to the surface. From this, the normal force due to the deflected stream can be calculated for the next increment as shown in Figure 3. Hence, in general when the average normal for the previous increment is ϕ_{i-1}, and that of the increment being considered ϕ_i, the rate of momentum in the stream leaving parallel to the element, S_i, would be:

$$S_i = S_{i-1}Cos(\phi_i - \phi_{i-1}) - S_r Sin\phi_i \quad . \tag{23}$$

The normal force on the element would be:

$$dF_i = S_{i-1}Sin(\phi_i - \phi_{i-1}) + S_r Cos\phi_i \quad . \tag{24}$$

For this general element the rate of momentum in the stream S_r is:

$$S_r = \frac{m^2(X_i^2 - X_{i-1}^2)}{\pi DR^4} \tag{25}$$

During the actual integration, the final X coordinate, the amount of surface areas, ds, and the average normal angle, ϕ_i, for a general element are unknown. Initial estimates were used in Equations 23-25 to calculate the $\frac{b}{T}\left(\frac{dF}{ds}\right)$ term. The set of Equations 9-14 were then integrated for a

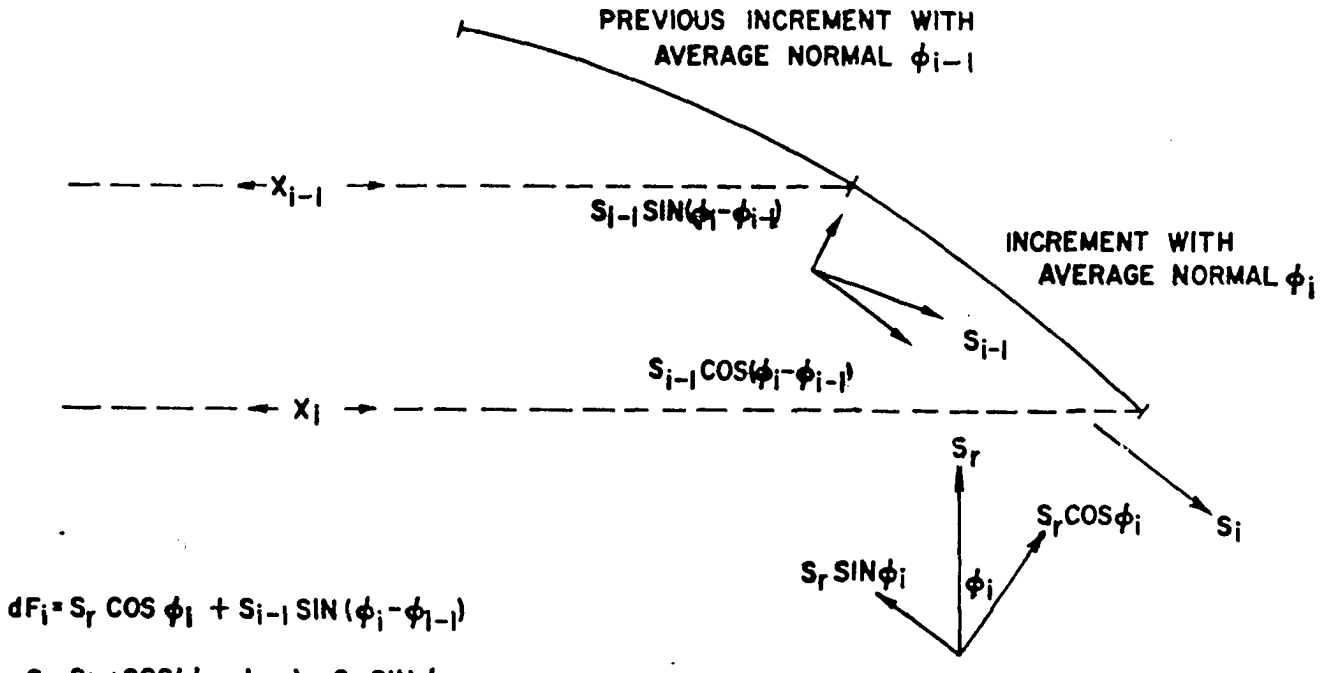

$$dF_i = S_r\,COS\,\phi_i + S_{i-1}\,SIN\,(\phi_i-\phi_{i-1})$$

$$S_i = S_{i-1}\,COS(\phi_i-\phi_{i-1}) - S_r\,SIN\,\phi_i$$

$$S_r = \frac{m^2(x_i^2 - x^2_{i-1})}{\pi DR^4}$$

Figure 3. Momentum balance on the ith increment

preset distance along the interface. The initial estimates were compared with the actual values and if any of the assumed values were in error by more than 0.1%, new estimates were made and the integration of the increment repeated. This process was continued until the entire profile was determined.

The magnitude of the normal force due to the deflected stream was always considerably less than that due to the stream coming directly from the orifice. When the calculated momentum component, S_i, of the deflected stream became negative, the associated force term was neglected. If S_i is negative, this tends to indicate that the deflected stream was now moving up rather than down the interface of the droplet. This condition would require a much more elaborate integration scheme than developed for this problem.

Since the force due to the stream S_r becomes zero when the X coordinate exceeds the radius of the origin, the integration proceeds more rapidly as the profile is developed. No iteration scheme is necessary if X is greater than R and the force due to S_i may be neglected.

Separating Droplet - First Stage

The equations which describe the forming droplet are very restricted since they apply only as long as the volume is less than the critical value. Above this volume, a new equation is needed which will apply to the profile. If an equation were available which described the profile of a droplet having no flow effects but with a volume larger than the critical value, an effort could be made to add the effect due to fluid flow in a manner similar to that done with the equations of Laplace.

When the volume is larger than the critical value, a portion of the droplet will separate from the plate even though there is no flow into it. Near the critical value, the droplet is extremely stable and may require more than five minutes to complete the separation process. A droplet in which all of the flow effects due to formation are negligible and which has a volume only slightly larger than the critical value will be called a separating droplet.

The basic approach which was used to derive the equation applying to the static case should be useful in describing a separating droplet. If axial symmetry and constant surface tension are assumed, the pressure term of Laplace and the equations of Bashforth and Adams may be used once a suitable pressure balance across an element of interface is developed.

During the separation process the pressures acting on an element of surface must be slightly out of balance. The pressure due to surface curvature will vary as the separation proceeds since the sum of the two radii of curvature will change as the profile changes. The hydrostatic pressures acting on the element due to the two fluids will also change as the height of the droplet varies. Since these last two pressures may be expressed as linear functions of $\bar{Z}$, this suggests the assumption that the difference in pressure across the element is also a linear function in $\bar{Z}$. If this assumption is made, a pressure balance across an element of interface would be of the form:

$$e + c\bar{Z} = p + T\left(\frac{\sin\phi}{\bar{X}} + \frac{1}{\rho}\right) - P \quad . \tag{26}$$

This expression may be simplified and rearranged so that it may be conveniently used with the equations which result from the assumption of

axial symmetry. Equations 4 and 5 which express P and p in terms of their values at the origin may be substituted into Equation 26.

$$e + c\bar{Z} = p_o + dg\bar{Z} + T\left(\frac{\mathrm{Sin}\phi}{\bar{X}} + \frac{1}{\bar{\rho}}\right) - P_o - Dg\bar{Z} \tag{27}$$

This equation may be evaluated at the origin:

$$e = p_o + \frac{2T}{b} - P_o \ , \tag{28}$$

and this result used to eliminate e, P_o and p_o from Equation 27:

$$\frac{2T}{b} + c\bar{Z} = dg\bar{Z} + T\left(\frac{\mathrm{Sin}\phi}{\bar{X}} + \frac{1}{\bar{\rho}}\right) - Dg\bar{Z} \ . \tag{29}$$

Finally, the dimensionless groups and coordinates may be used to express the equation in a form which may be combined with Equations 12-14.

$$\frac{1}{\rho} = 2.0 + \beta Z + \frac{cb^2 Z}{T} - \frac{\mathrm{Sin}\phi}{X} \tag{30}$$

The initial conditions for this integration are the same as those listed in Equations 15-17.

Equation 30 is the same as the static equation when the term containing c is neglected. The function of the parameter c in the equation can be understood clearly in terms of its interaction with the parameter β.

As the droplet grows the value of β increases until the critical volume is reached. At this point, any further increase would require a decrease in the volume of the droplet. However, the shape of the profiles for larger values indicates that β must continue to increase if the droplet is to separate. Since β and (cb^2/T) are of the same form, the addition of the parameter c permits β to continue to increase, allowing the separation process to continue while c compensates for this increase and

satisfies any necessary volume requirements. For a separating droplet, the parameter c would be chosen such that the volume of the droplet remained a constant.

The equations containing the parameters were programmed using the computer such that the value of c could be easily iterated with respect to the volume of the droplet at the end of the integration. β was then increased from its value at the critical volume and c determined such that the volume under the curve was equal to that measured at the start of the separation. This permitted the profiles of a droplet of constant volume to be determined for increasing values of β.

An additional assumption of this model is that the fluid surrounding the droplet offers negligible resistance other than that of hydrostatic pressure to the change in shape of the profile. As long as the separation process is proceeding slowly, this assumption should be reasonable. However, once the droplet begins to have a minimum in the profile, the rate of the process rapidly increases. At this point, photographs of the droplet show that the initial curvature stops decreasing and begins to increase. One possible effect which might become significant is the resistance of the surrounding fluid.

Separating Droplet - Second Stage

In order to include the resistance of the surrounding fluid to changes in the shape of a separating droplet, assumptions must be made concerning the motion of the droplet and the path of the flow around the profile. As a first approximation, the portion of the droplet above the minimum or neck of the profile was assumed to be moving upward as a unit. The

upward velocity of this portion may change during the separation process.

The surrounding fluid which was displaced by this upward motion was assumed to flow parallel to the profile and impinge against the base of the droplet with the same downward velocity (Figure 4). This model is very approximate but it should assist in determining if the resistance of the surrounding fluid is the additional effect needed to generate computed profiles which are similar to those observed experimentally.

The magnitude of this resistance on an element of the interface located above the neck of the droplet will depend on the upward velocity and the normal angle of the element. When V is the velocity and ϕ is the angle, the resistance would be:

$$\left(\frac{dF}{ds}\right) = V^2 d \cos^2 \phi \quad . \tag{31}$$

At the apex of the droplet (ϕ=o), this pressure would be:

$$\left(\frac{dF}{ds}\right)_o = V^2 d \quad . \tag{32}$$

This resistance may be added to the force balance of Equation 26.

$$e + c\bar{Z} + P = p + T\left(\frac{\mathrm{Sin}\phi}{\bar{X}} + \frac{1}{\rho}\right) + \left(\frac{dF}{ds}\right) \tag{33}$$

At the apex:

$$e + P_o = p_o + \frac{2T}{b} + \left(\frac{dF}{ds}\right)_o \quad . \tag{34}$$

Equations 31-34 may be combined and the result expressed in terms of dimensionless variables.

$$\frac{1}{\rho} = 2.0 + \beta Z + \frac{cb^2}{T} Z - \frac{\mathrm{Sin}\phi}{X} + \frac{V^2 bd}{T} - \frac{V^2 bd \mathrm{Cos}^2 \phi}{T} \tag{35}$$

This equation along with those resulting from the assumption of axial

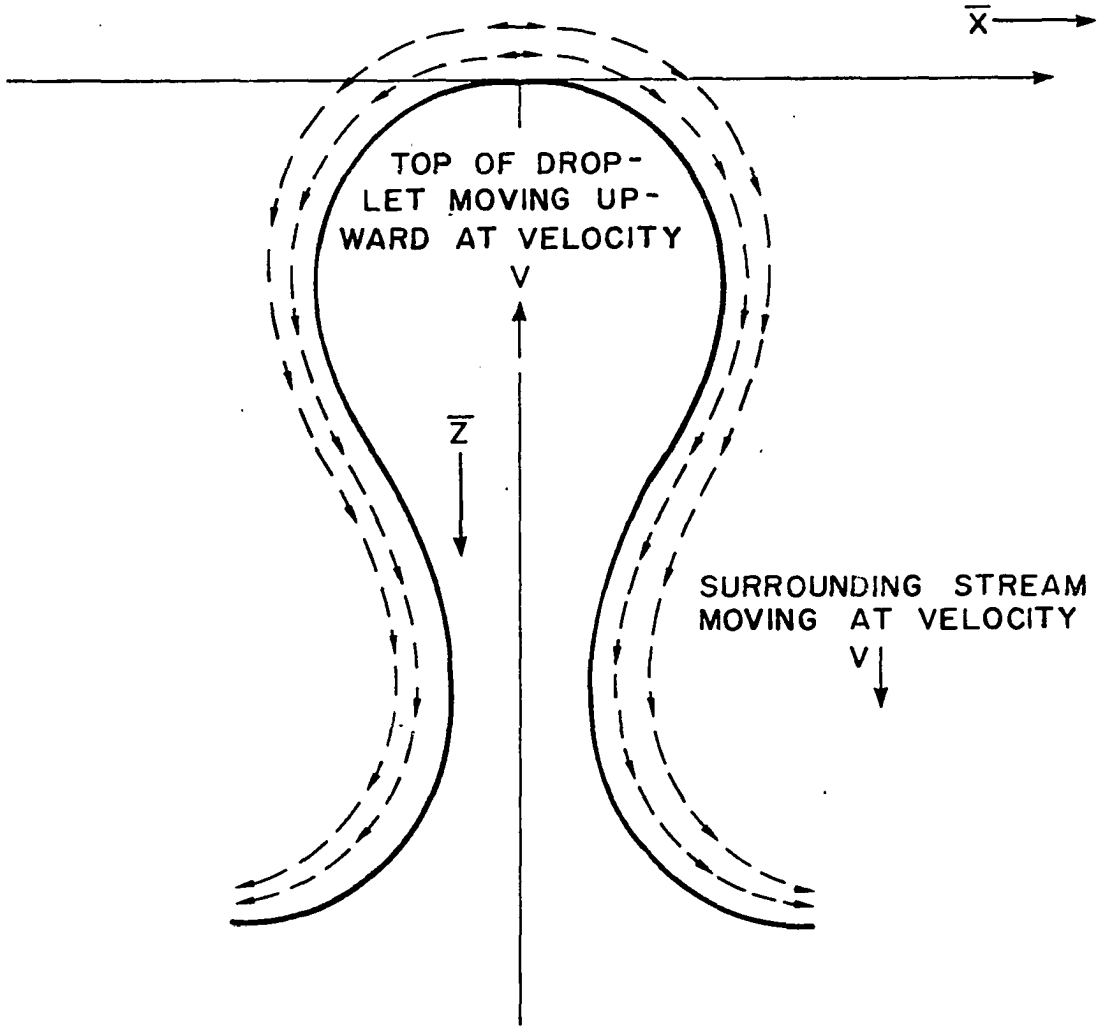

Figure 4. Assumed motion of the droplet during the final stage of separation

symmetry may be integrated to obtain the top of the profile until the normal angle exceeds 90 degrees. At this point, the last term in Equation 35 which represents the inward pressure due to the surrounding fluid, must be omitted since any surface elements with normals greater than 90 degrees are assumed to have fluid flowing only parallel to them.

The integration may be continued until the minimum or neck in the profile is reached and the normal angle again becomes less than 90 degrees. The term representing the resistance of the surrounding fluid should again be included in the equation. Also, an additional pressure not included in Equation 35 must be included in the force balance on an element of interface located below the neck of the droplet. As the fluid flows parallel to the profile in this region, it is diverted slightly from its path. This is analogous to one of the pressures involved in a forming droplet. The expression for S_i in this case would be:

$$S_i = S_{i-1} \operatorname{Cos}(\phi_i - \phi_{i-1}) + \frac{V^2 bd}{T} \operatorname{Sin}\phi_i \operatorname{Cos}\phi_i \tag{36}$$

$$S_1 = \frac{V^2 bd}{T} \tag{37}$$

$$dF_i = \frac{V^2 bd \operatorname{Cos}^2 \phi_i}{T} + S_{i-1} \operatorname{Sin}(\phi_i - \phi_{i-1}) \tag{38}$$

Using these equations profiles of droplets of a known volume may be generated by varying the two parameters β and V. When V is assumed to be zero the equations reduce to those applying to the separating droplet.

EXPERIMENTAL PROCEDURE

Photographs of droplets growing on a submerged plate were taken using a 4X4X8 inch Plexiglas chamber. The front of this chamber could be easily removed and a new plate of either a different orifice size or a different material could be inserted. The chamber was made this large in order to minimize wall effects on the profile.

The droplets were composed of a 2:1 mixture of mineral oil and Varsol*, which was water saturated. The surrounding fluid was distilled water which was saturated with the mineral oil-Varsol mixture. This system was chosen because of ease of handling and the size of the droplets formed on a submerged plate. The interfacial tension was measured using a Du Nuoy tensiometer and varied slightly from batch to batch but was approximately 50 dynes/centimeter. The specific gravity of the mineral oil-Varsol phase was about 0.84 and that of the saturated water phase approximately 0.99. The viscosity of the light phase was about 7 centipoise. All of these were measured at 25 degrees centigrade. When runs were made, the two feeds were maintained at 25°C using a constant temperature bath and the room temperature was also set at this value.

A schematic of the drop growing apparatus and a photograph are shown in Figures 5 and 6. In order to photograph the droplets, a plate of the desired material and orifice size was placed in the chamber. The lower portion of the chamber was filled with the mineral oil-Varsol mixture and then the upper portion filled with saturated water. After the hypodermic

---

*Varsol is a purified fraction of C_9 and C_{10} hydrocarbons sold by the Humble Oil and Refining Company.

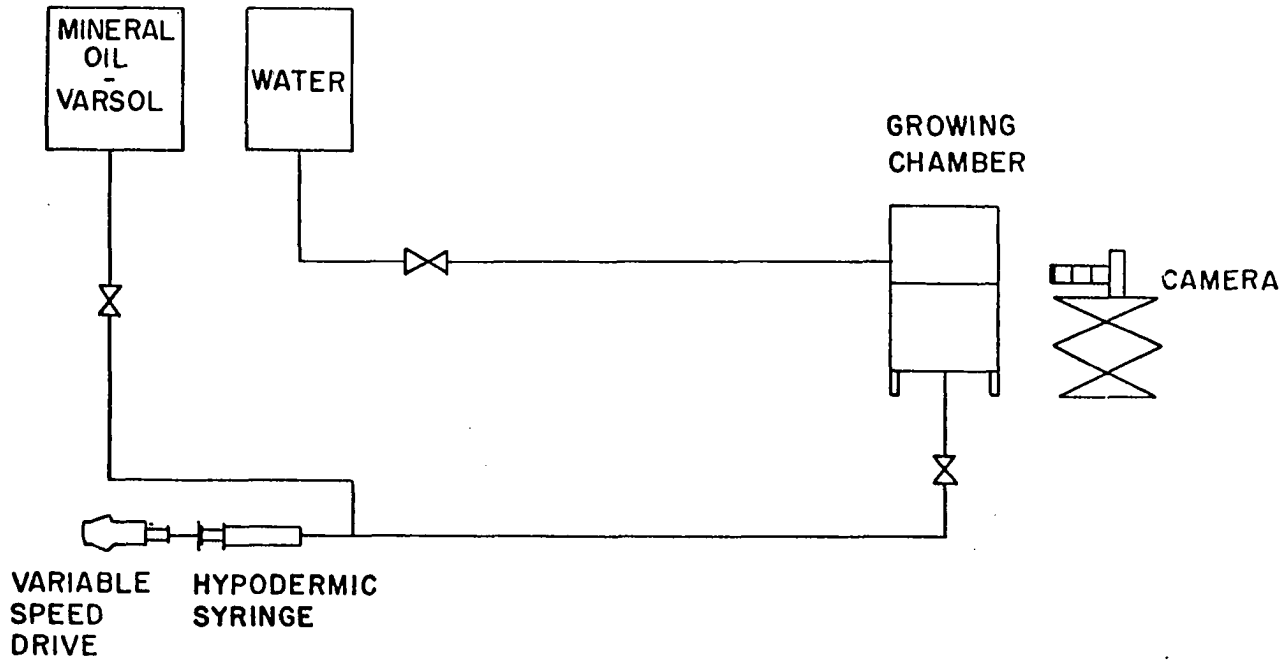

Figure 5. Flow diagram of the drop formation equipment

Figure 6. Photograph of the drop formation equipment

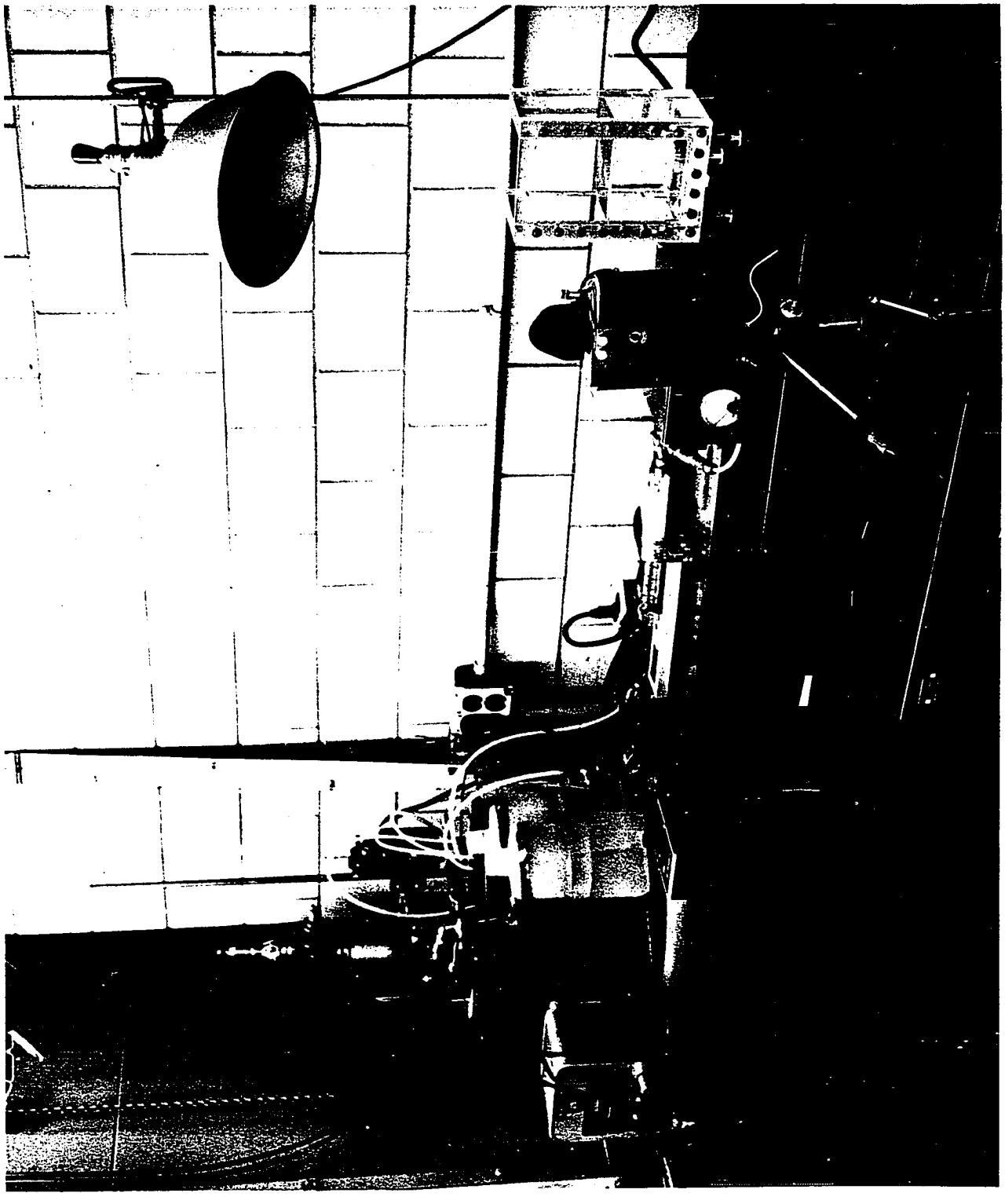

syringe had been filled with mineral oil-Varsol, droplets could be grown at varying flow rates using the variable speed drive.

The photographs of a forming droplet were taken using a motorized Leica M2 camera and those of a separating droplet by a Kodak-Cine movie camera. An object of known size was placed in the chamber so that the profiles could be measured from enlargements. Typical photographs of droplets forming on a stainless steel and a Teflon plate are given in Figures 7 and 8. These figures indicate that the angle of contact between the interface and the Teflon plate is difficult to determine while the contact angle for the stainless steel plate is quite clear.

Figure 7. Photograph of a droplet forming on a stainless steel plate, orifice diameter = 0.25 inch

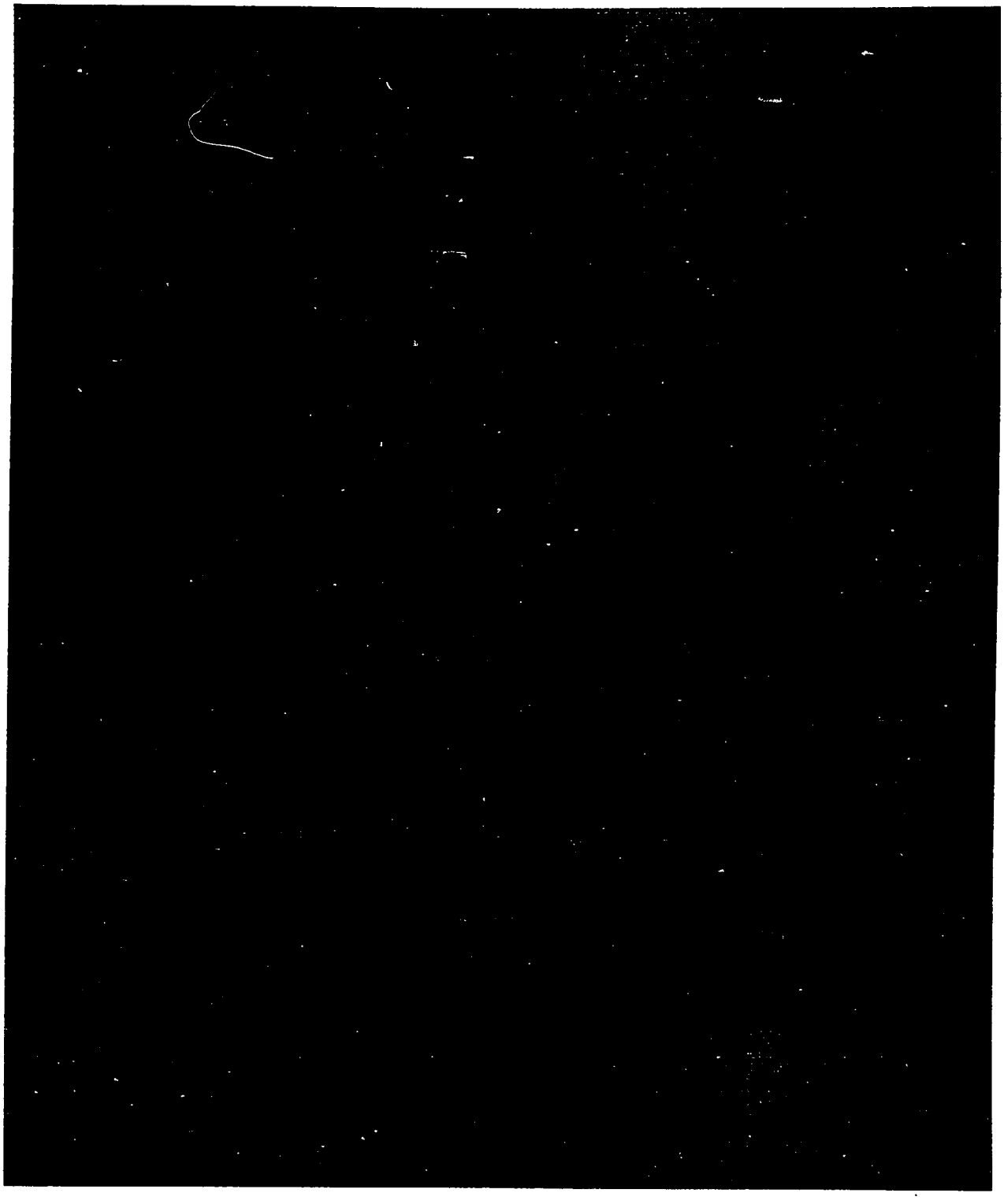

Figure 8. Photograph of a droplet forming on a Teflon plate, orifice diameter = 0.125 inch

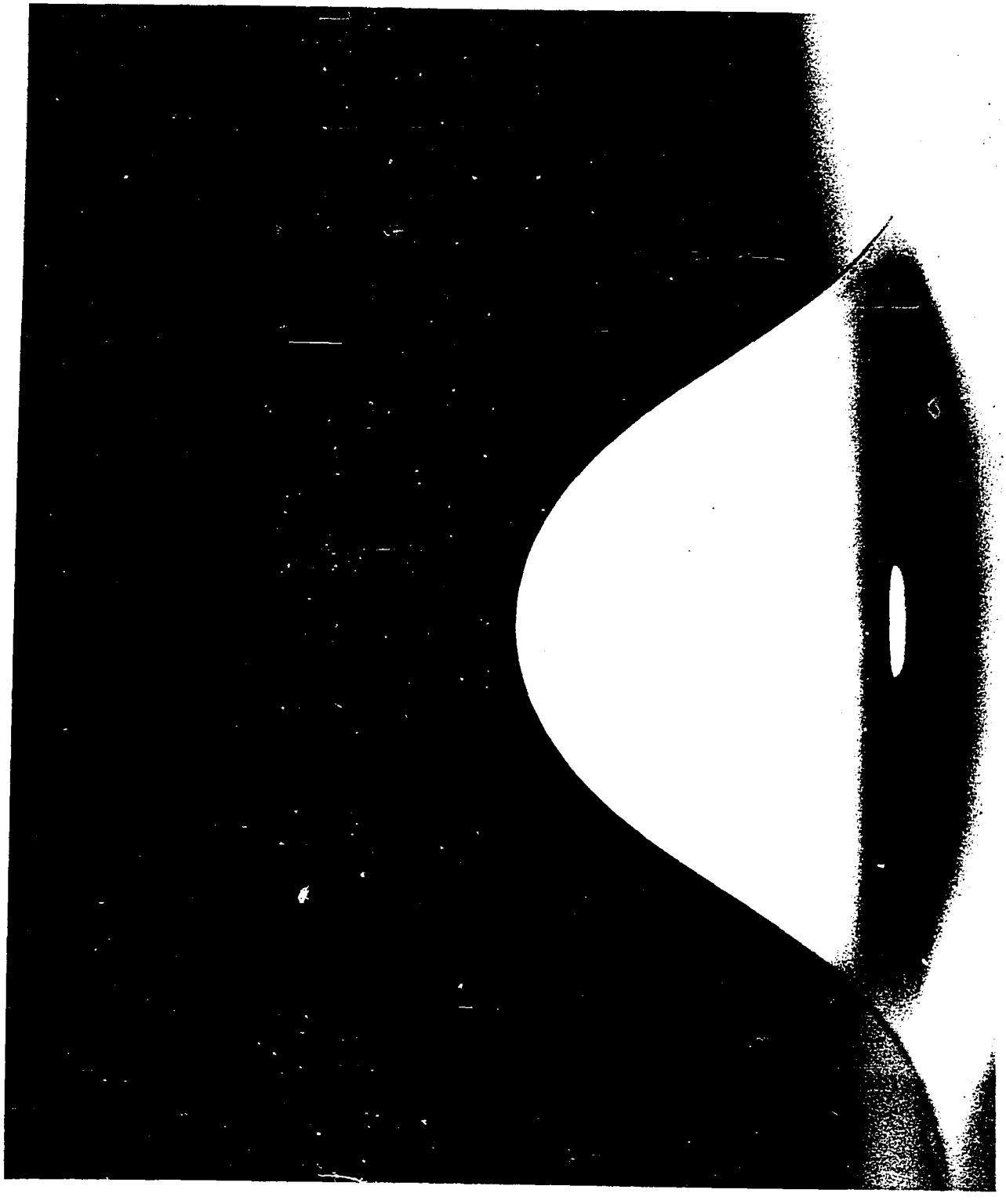

DISCUSSION OF RESULTS

Forming Droplet - Below Critical Volume

When the physical properties of the fluid, the orifice radius, and the mass flow rate into the droplet are all known, the only quantity needed to obtain a profile using Equations 9-14 is the initial curvature b. This is the quantity which changes as the droplet grows - decreasing as the volume increases until the critical volume is reached. Each particular droplet has associated with it a unique value of b. This value could not be determined with the desired accuracy from the photograph of the droplet. Therefore, the equations were integrated using several values of b to determine if there was a particular value which made the computed and experimental profiles similar in shape. This was the method used to determine how well the equations described the actual profiles.

Included in the parameter β is the interfacial tension between the two fluids. If mass-transfer were occurring, β would vary with any changes in the concentration at the interface. If the interfacial tension were a known function of droplet volume, surface area, or position on the surface, its variation could be included in the equations. However, this would make the integration more difficult and the determination of the required function would be difficult experimentally. Since the purpose of this study was primarily to investigate the accuracy of the dynamic terms, all of the data were taken using mutually saturated fluids and the tension was considered to be constant during the entire growth process.

When the equations are integrated, the initial curvature influences the shape of the profile through the dimensionless groups β and f. All of

the possible profiles which a droplet may assume can be generated by varying these two parameters. For a particular set of fluid properties, the profiles of droplets grown on the same type of plate maintain the same general shape as the flow rate increases because the value of b decreases to compensate for increases in the mass flow rate.

When the flow conditions are held constant, β increases to a maximum as the droplet grows to the critical volume. The magnitude of the values which β assumes during this type of growth depends upon the fluid properties and the initial curvature. The location of the range of values which β assumes during this growth may be changed by using either a different fluid system or a different plate material.

There are in general only two regions which produce droplets which have distinctly different profiles. These correspond to droplets which either spread out on the plate or those which do not wet the plate at all and have bases which are restricted to the orifice edge. Mathematically, one droplet is normally a single valued while the other is a double valued function at the critical volume.

As mentioned previously, these two types of droplets may be obtained experimentally by changing either the fluid system or the plate material. Since any change in the fluid system would introduce possible errors due to the measurement of fluid properties, only the plate material was changed. For the system used in this investigation a change from a Teflon to a stainless steel plate resulted in the desired change in profile.

When the Teflon plates were used, the droplet spread out on the plate and it was very difficult to determine experimentally whether the base of

the droplet was symmetric with respect to the orifice. If this were not so, the interface would no longer be a surface of revolution and one of the assumptions would be violated. The only means to check this was a careful examination of the photographs. In almost all droplets grown on this type of plate there would be some error due to this difficulty. Several different comparisons of the profiles of droplets grown on Teflon plates are plotted in Figures 9 through 11.

The effect of the dynamic terms on the solution can be seen in Figure 10 where the profile that results when these terms are neglected is also plotted. Another measure of the importance of the dynamic terms is the dynamic pressure f. An examination of Equation 9 indicates that if f is small relative to 2.0 then the dynamic terms can probably be neglected. For the flow conditions of the droplet in Figure 10, f was approximately 0.96.

Also plotted in Figure 10 as well as Figure 11 is the profile corresponding to the b value which compared to the experimental data if the static equation was used. As would be expected, the two families of curves for the static and dynamic cases are similar but Figure 11 indicates that the static equation is inadequate in this case.

Since the surface area and volume of static droplets have been tabulated, it would be desirable to use the static equation if possible. Practically, the static equation may be used as long as the value of the dimensionless group f is small compared to 2.0. In order to calculate f, a value of the initial curvature b is needed. This value may be obtained by estimating β and then calculating b, using Equation 10. For submerged

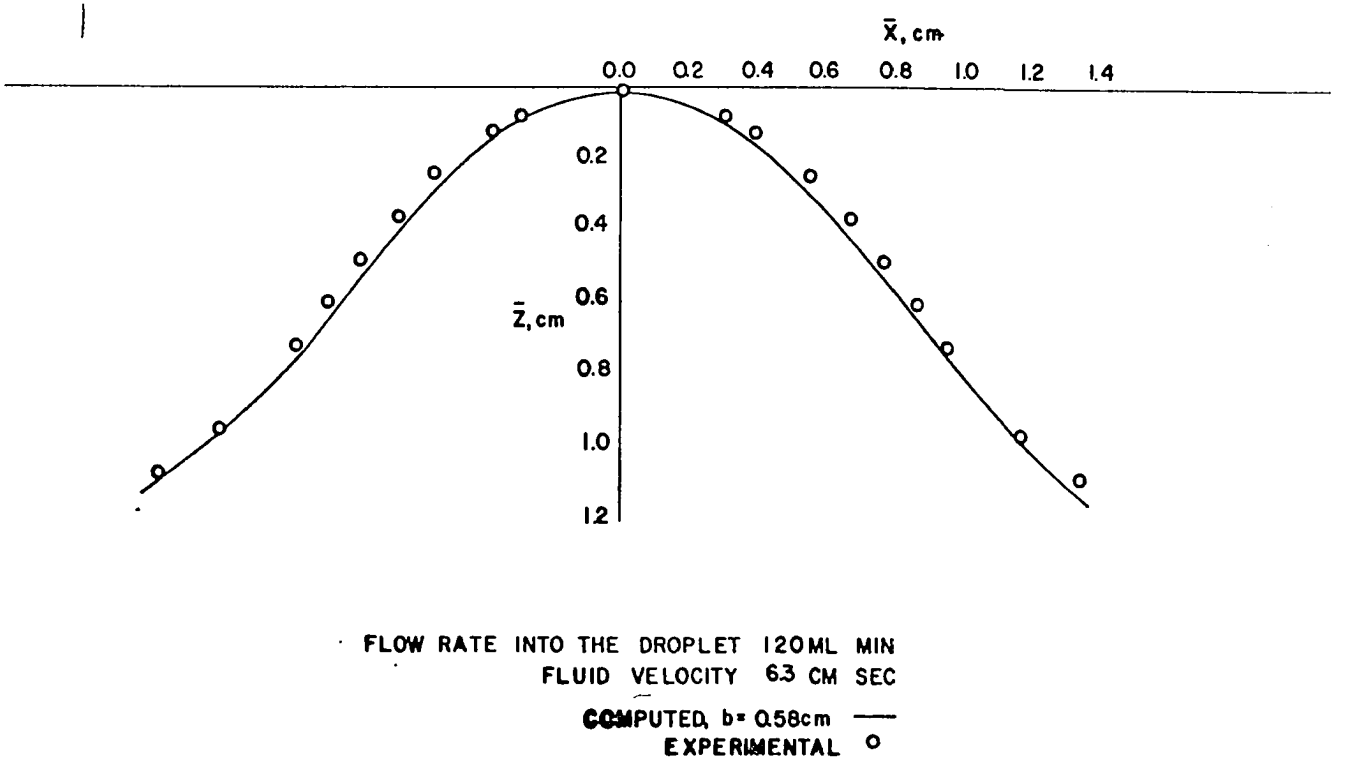

Figure 9. Comparison of profiles; Teflon plate, f = 0.39, orifice diameter = 0.25 inch

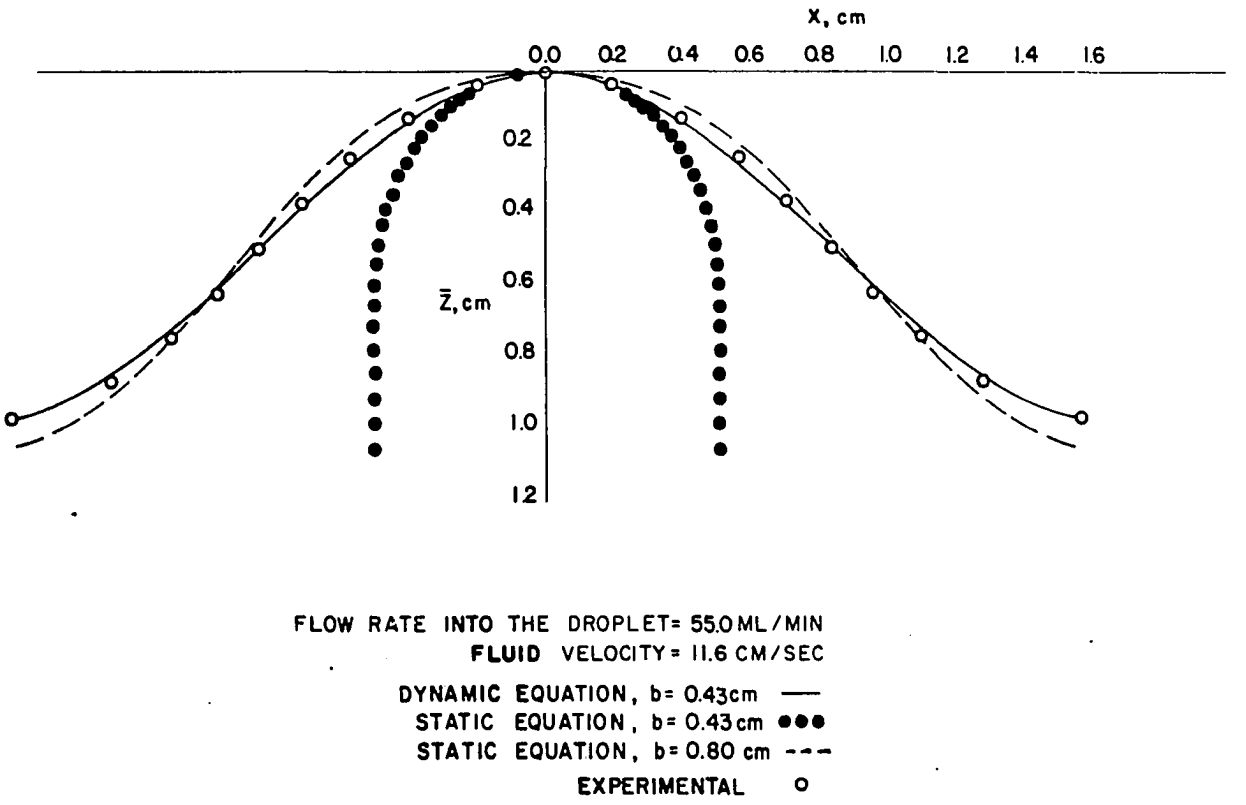

Figure 10. Comparison of profiles; Teflon plate, f = 0.96, orifice diameter = 0.125 inch

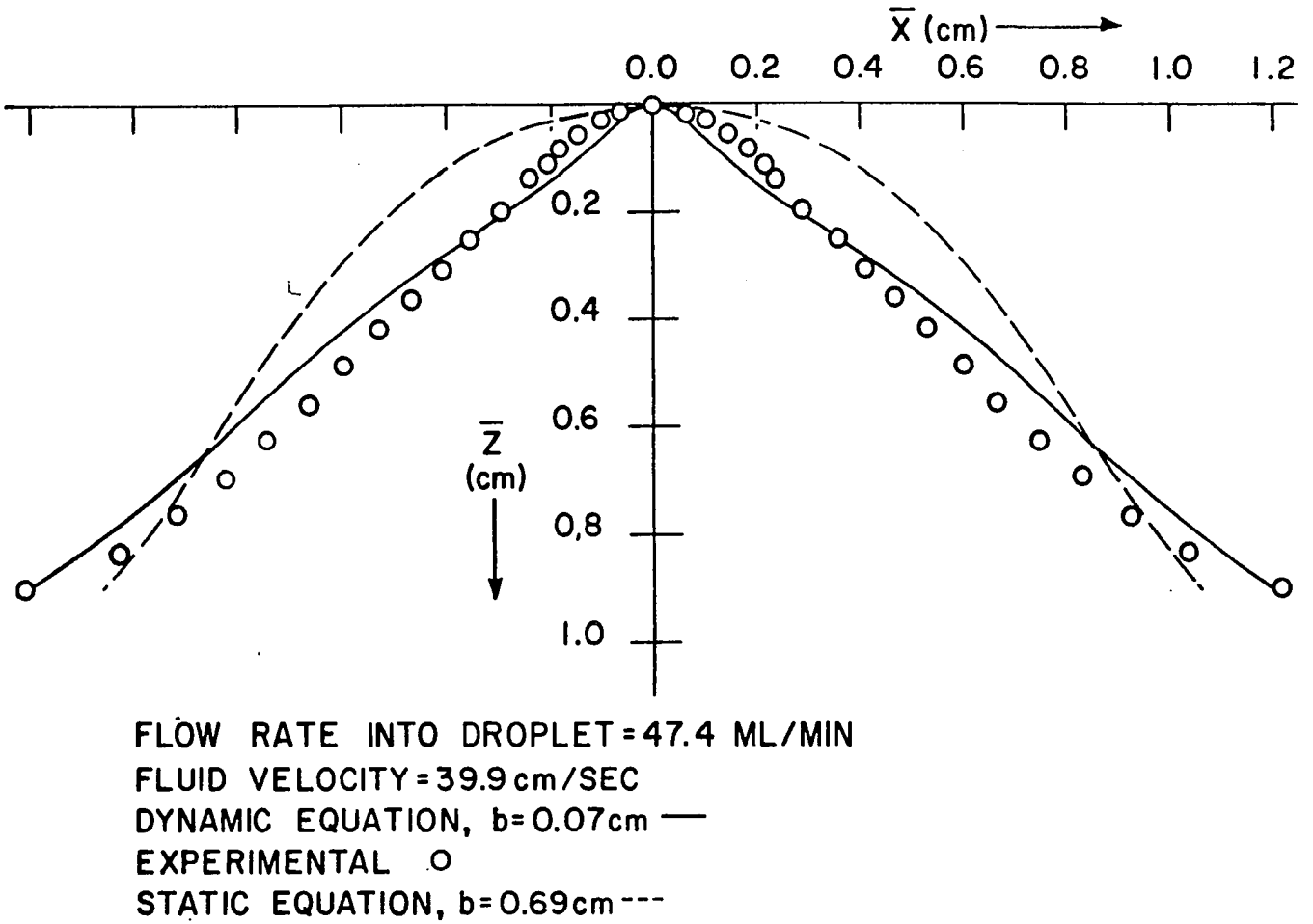

Figure 11. Comparison of profiles; Teflon plate, f = 1.82, orifice diameter = 0.0625 inch

sessile droplets, β is almost never less than -4.0 and may be assumed to be -1.0 if no other information is available. This should give a value of b which will probably be conservative for most droplets with a significant volume.

The droplet did not wet the plate at all when a stainless steel plate was used. Since the base of the droplet is determined by the edge of the orifice in this case, the interface will be a surface of revolution as long as the plate is level. The computed and experimental profiles of two droplets growing on this type of plate are compared in Figures 12 and 13.

The equations appear to provide a better description of droplets growing on this type of plate. This is probably due to the fact that these droplets more closely approximate a surface of revolution.

Separating Droplet - First Stage

It is experimentally difficult to form and photograph a separating droplet because it is necessary to form the droplet slowly in order to minimize any flow effects. The critical volume should be exceeded by as little as possible because when the volume becomes too great, the droplet will be well into the separation process before the flow effects become negligible. Also, since the volume under the curve is assumed to be a known value it is convenient to stop as closely as possible to the critical value.

Although the Varsol-mineral oil-water system formed droplets which were easy to photograph, it was difficult to determine the volume of a droplet at the start of separation when a Teflon plate was used. In order to determine the critical value, it is necessary to know the angle of

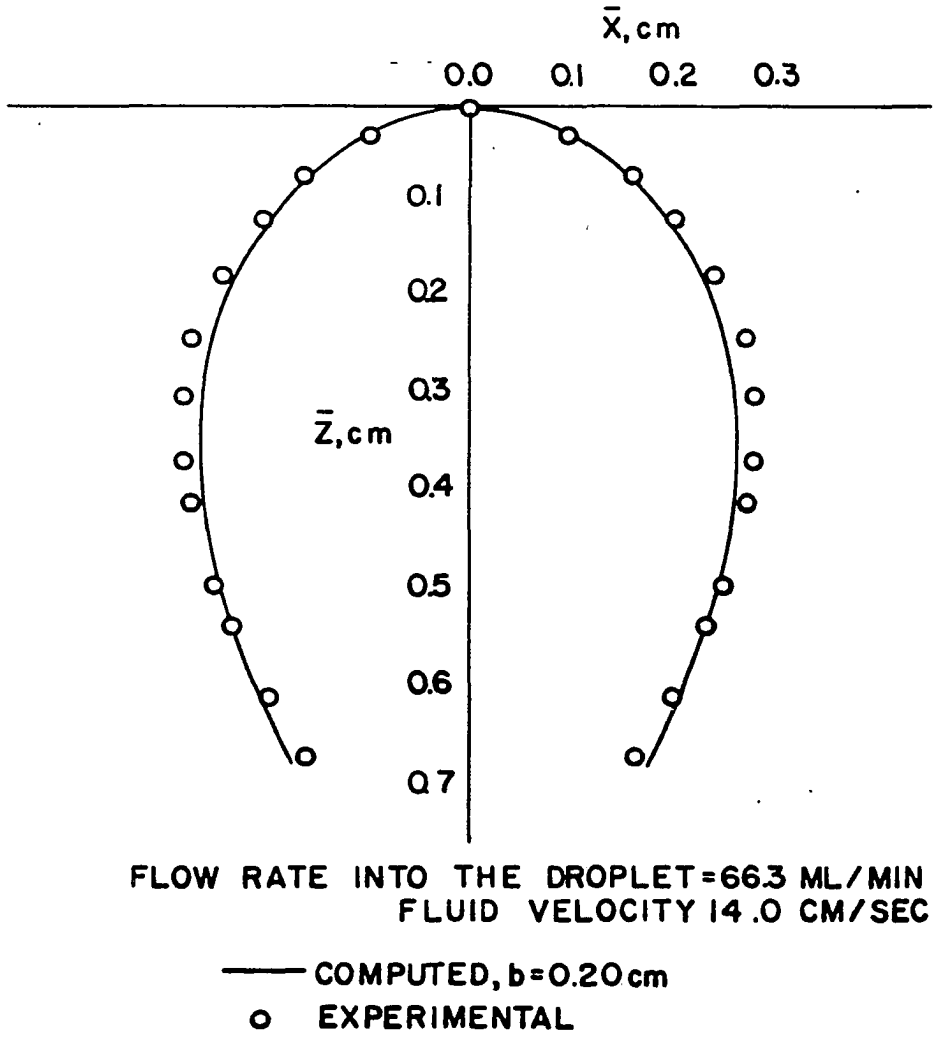

Figure 12. Comparison of profiles; stainless steel plate, f = 0.65, orifice diameter = 0.125 inch

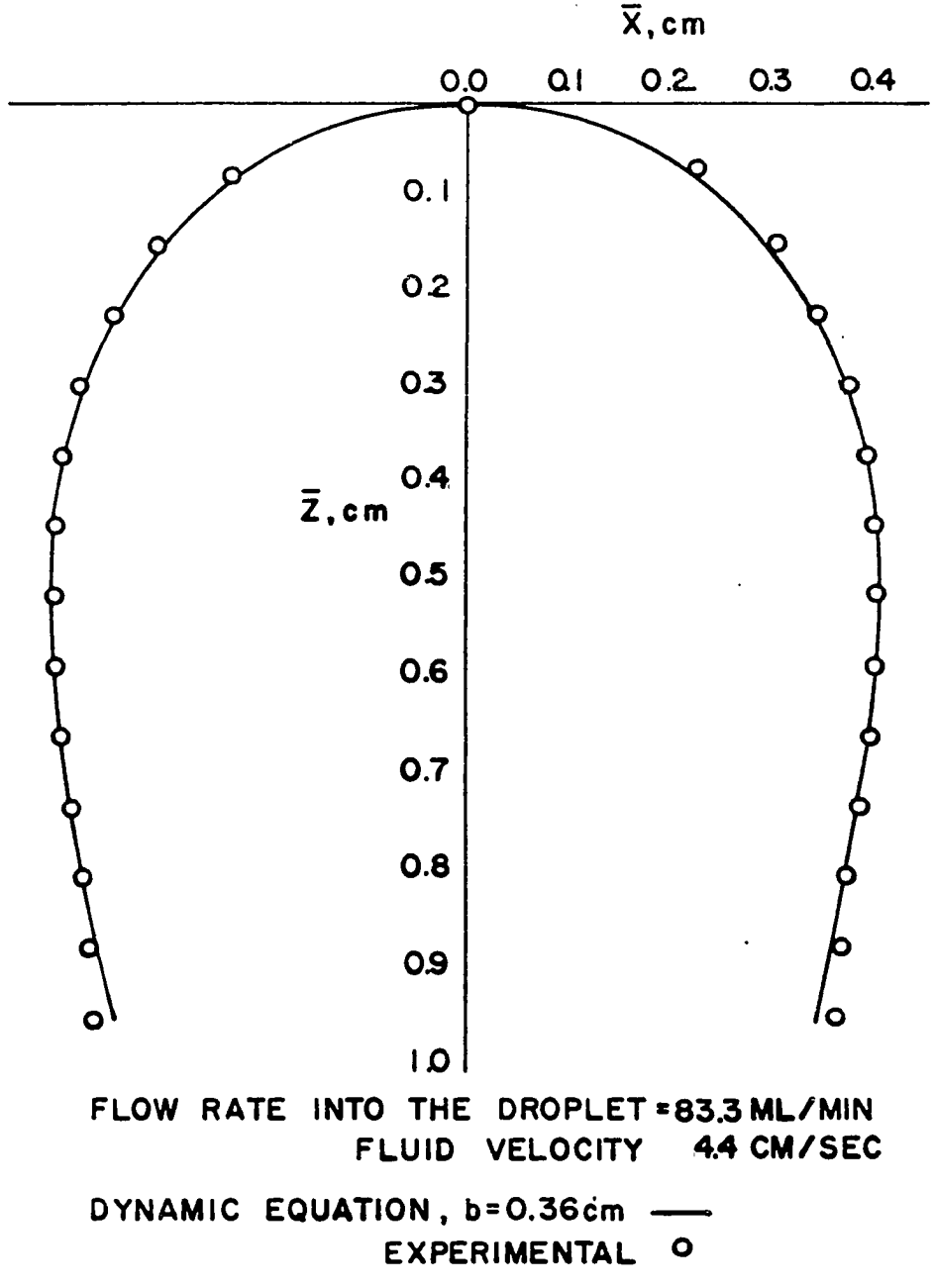

Figure 13. Comparison of profiles; stainless steel plate, f = 0.12, orifice diameter = 0.25 inch

contact between the drop interface and the surface of the plate. This angle, which could be used as a boundary condition to stop the integration, appears to depend on the condition of the plate and is difficult to measure accurately.

When the droplet rested on a Teflon plate, this measurement was almost impossible since the angle is very small and the interface not distinct just above the plate. Because of this difficulty for Teflon plates, the volume of the droplet at the start of the separation was obtained by comparing the initial profile to static profiles of known volume. Since receding contact angles are normally less than advancing contact angles, the angle between the profile and the plate was assumed to be zero in order to develop the computed profiles for a separating droplet.

Although droplets may require up to five minutes before complete separation occurs, the profile is changing so rapidly at the end of this process that a movie camera running at 64 frames per second does not adequately record the separation. Because of the amount of film used at this rate is was necessary to run the camera intermittently. Frequently, the end of the separation would take place so rapidly than an observer could not respond quickly enough to start the camera.

A sequence of profiles obtained from greatly enlarged motion picture frames of a separating droplet is shown in Figures 14 through 19. The first profile was measured immediately after the flow into the droplet had stopped. The computed volume under the static profile is 3.27 milliliters.

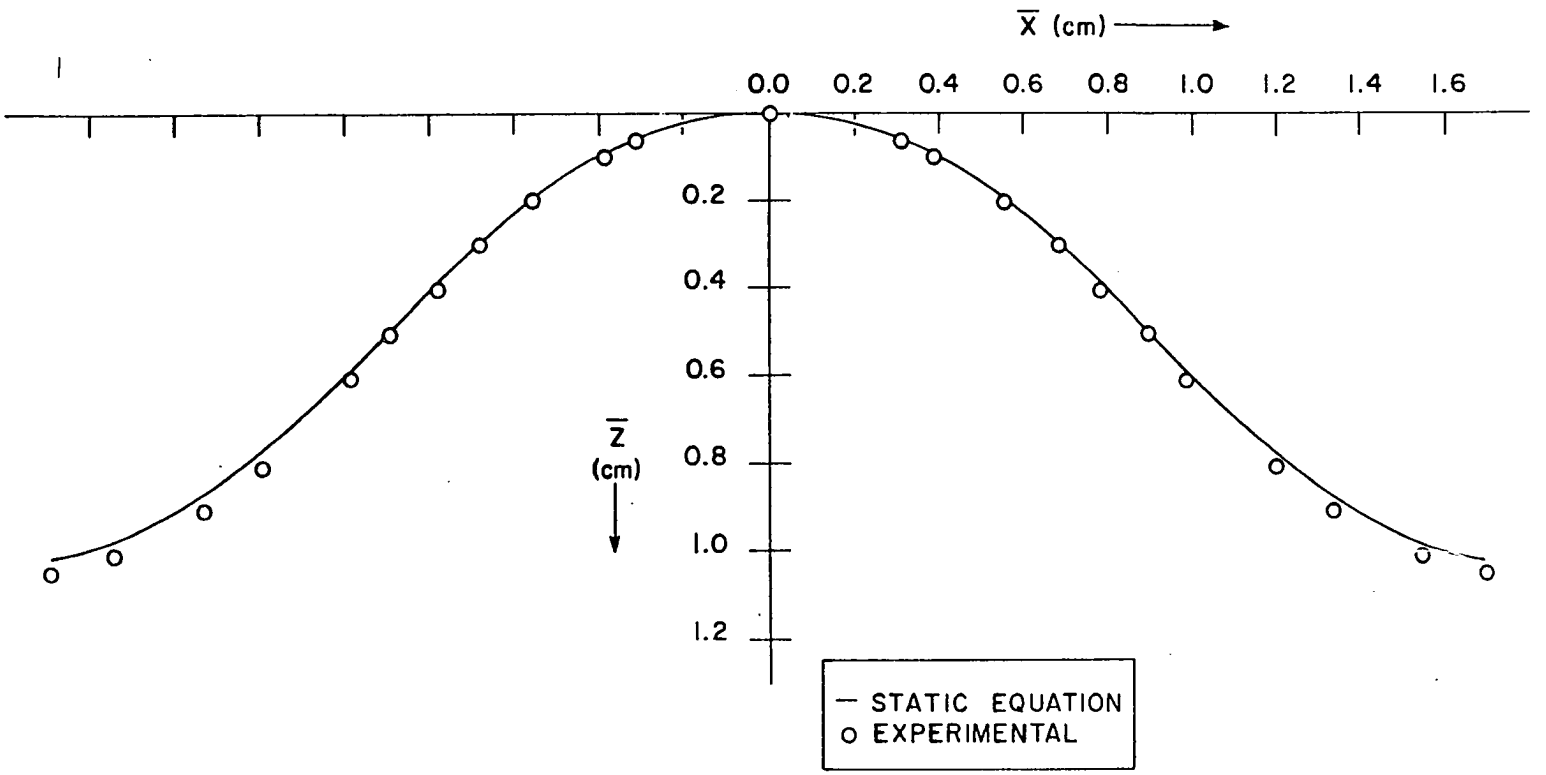

Figure 14. Initial profile of the droplet at the start of separation

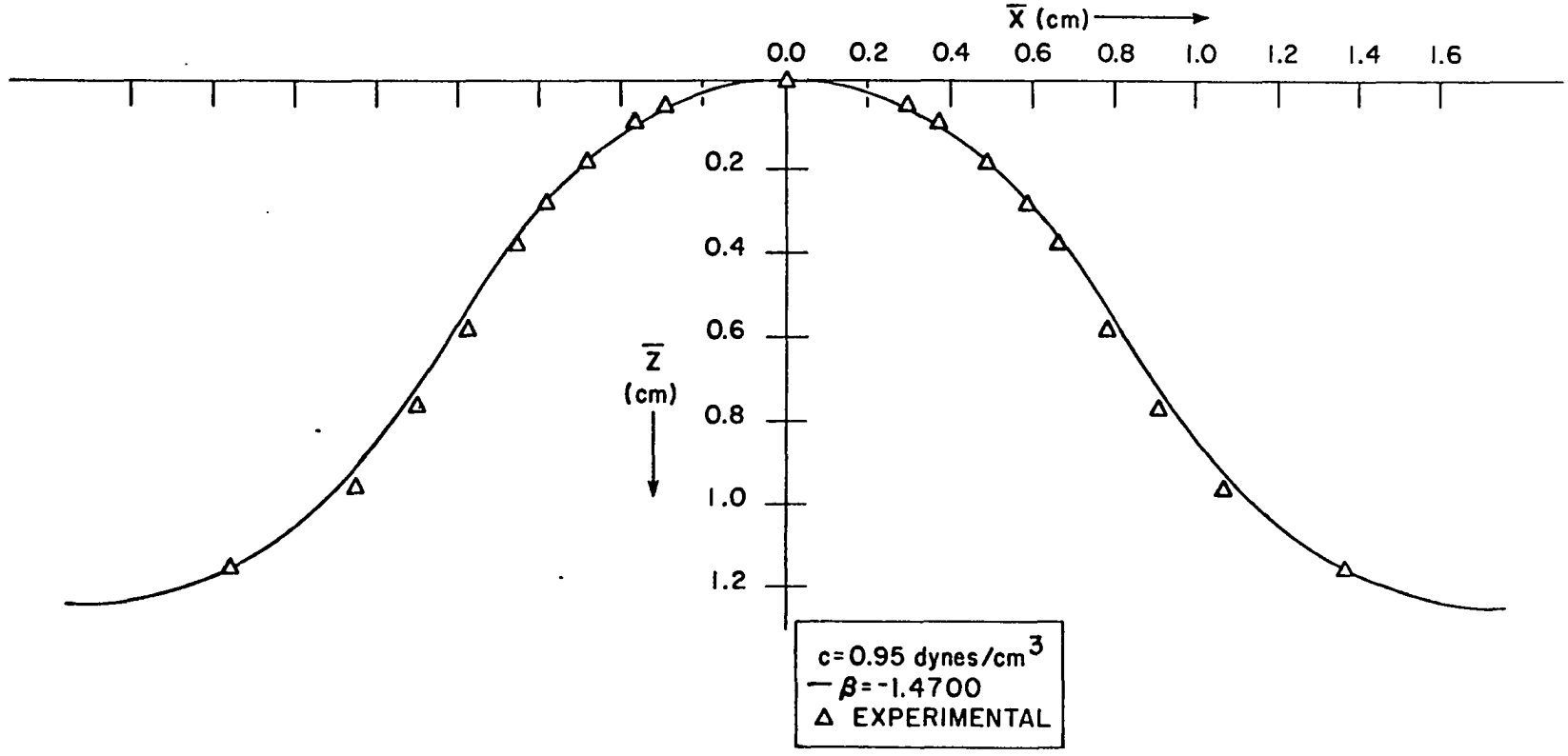

Figure 15. Profile of the droplet after the separation process has begun

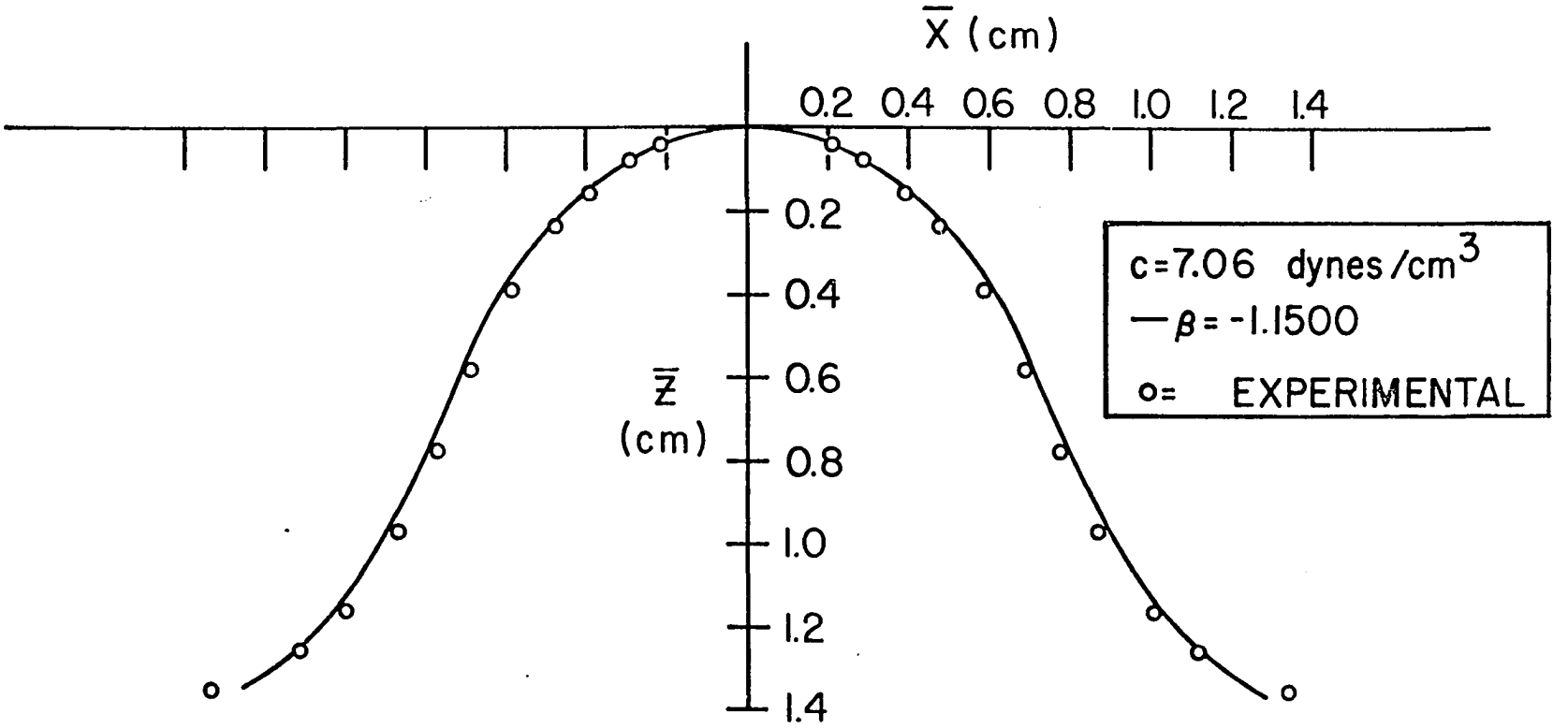

Figure 16. Profile of the droplet during the initial stages of separation

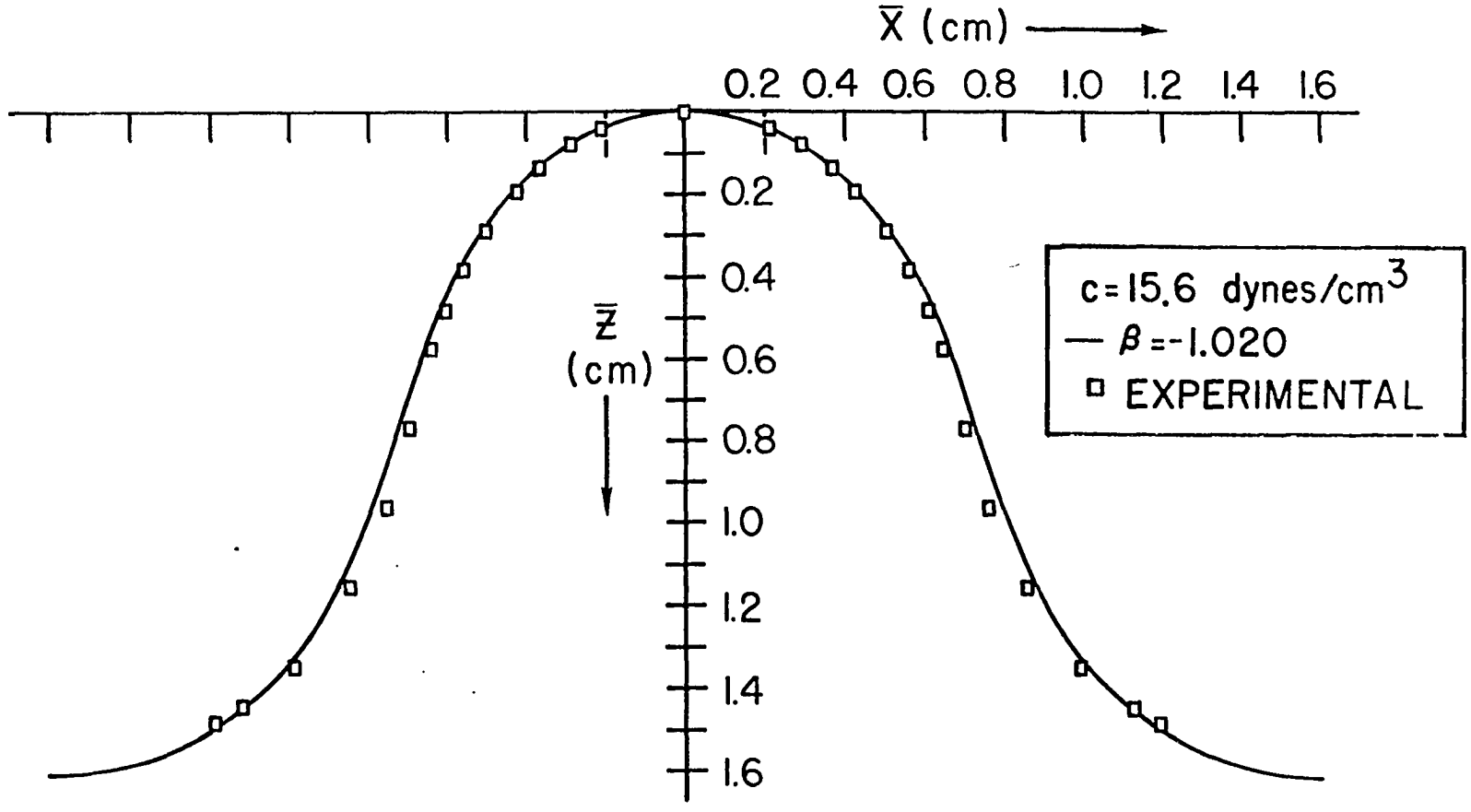

Figure 17. Profile of the droplet near the midpoint of the first stage of separation

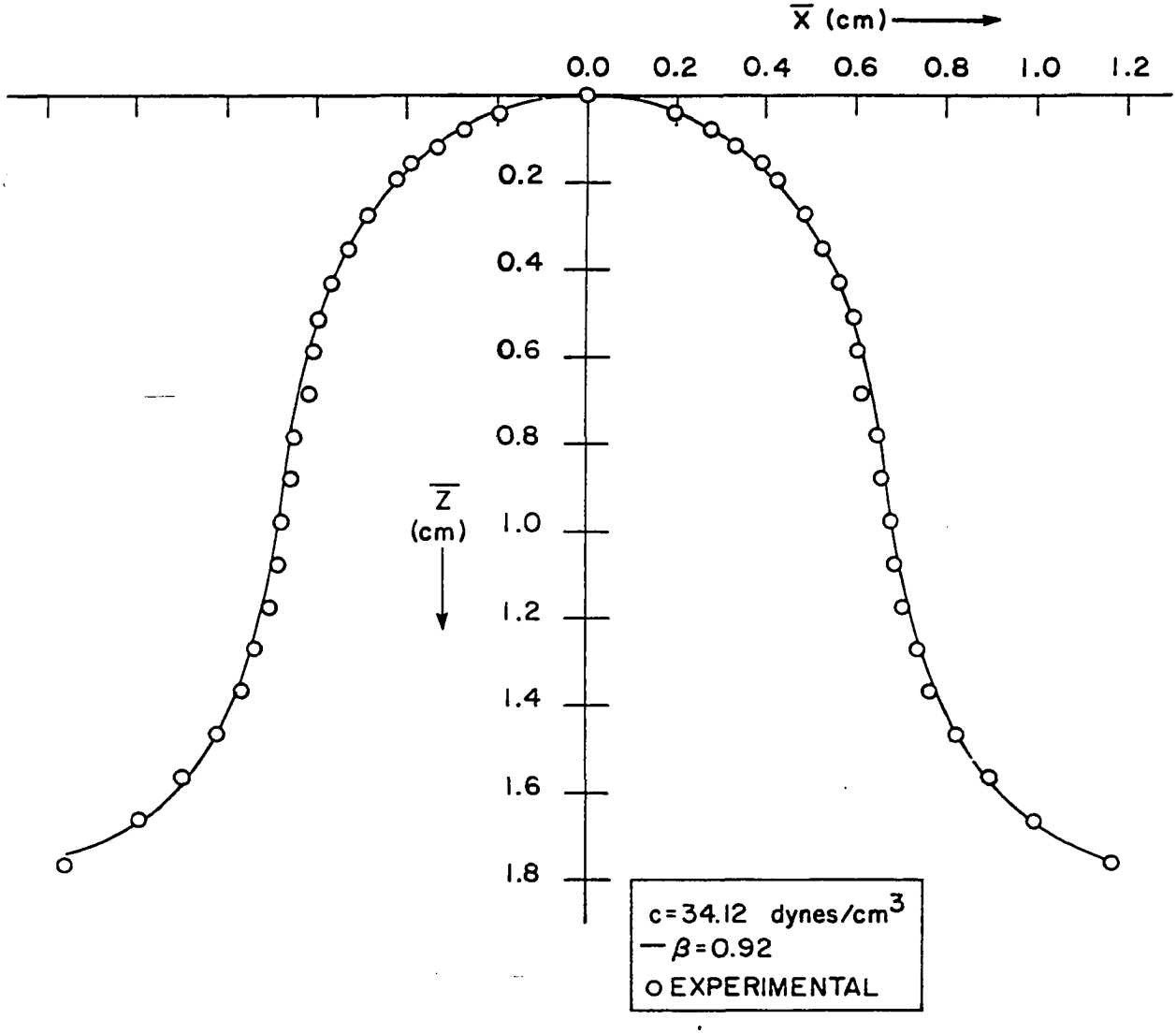

Figure 18. Profile of the droplet near the end of the first stage of separation

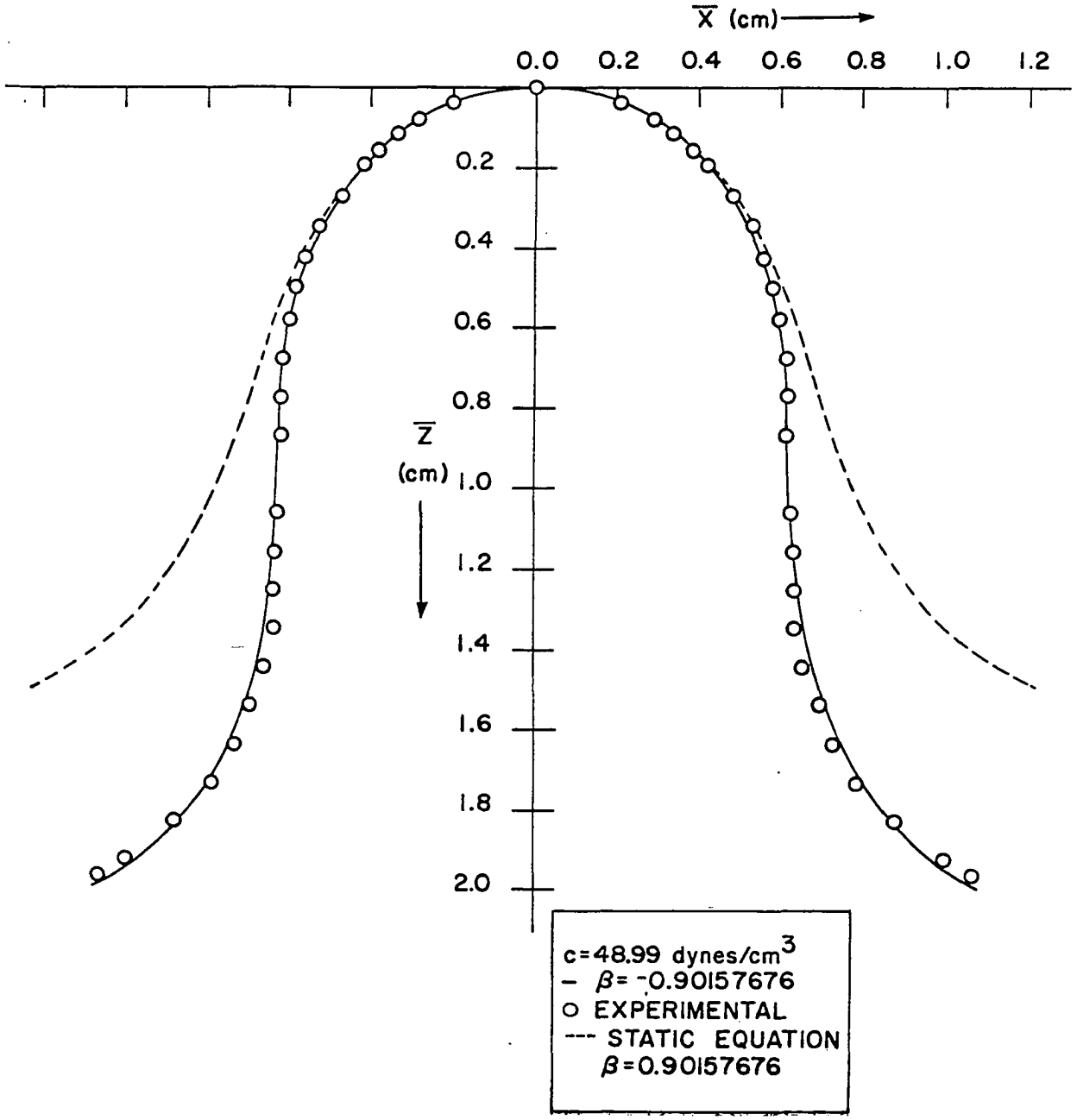

Figure 19. Profile of the separating droplet at the end of the first stage of separation

When the volume is known, a one parameter family of curves may be generated by varying β using the model developed for a separating droplet. The model was used to find a member of this family which was similar to each of the profiles in the sequence. The agreement between the experimental and computed profiles appears to improve as the separation proceeds.

These profiles are of a droplet of the mineral oil-Varsol-water system resting on a Teflon plate. When a stainless steel plate is used the profile already has a minimum at the critical volume and β appears to start decreasing immediately when separation begins.

The last profile in the sequence, Figure 19, also contains a plot of the solution to the equations if the term containing the volume parameter, c, is omitted. This indicates that this parameter is significantly influencing the shape of the profile. The droplet began to have a minimum or neck almost immediately after this last profile was measured.

A plot of $(\frac{cb^2}{T})$ versus β shows another reason why a new model is needed to describe the droplet after the last profile in this sequence. The value of the parameter for the last profile is the maximum on Figure 20 and the slope at this point indicates that some new effect is needed to continue the separation process. The large slope also means that the pressure drop across the interface would have to become very large in order to continue the separation process. Using the computer, values of the volume parameter c may be found when β is less than 0.90, but the computed profiles do not correspond to any observed experimentally.

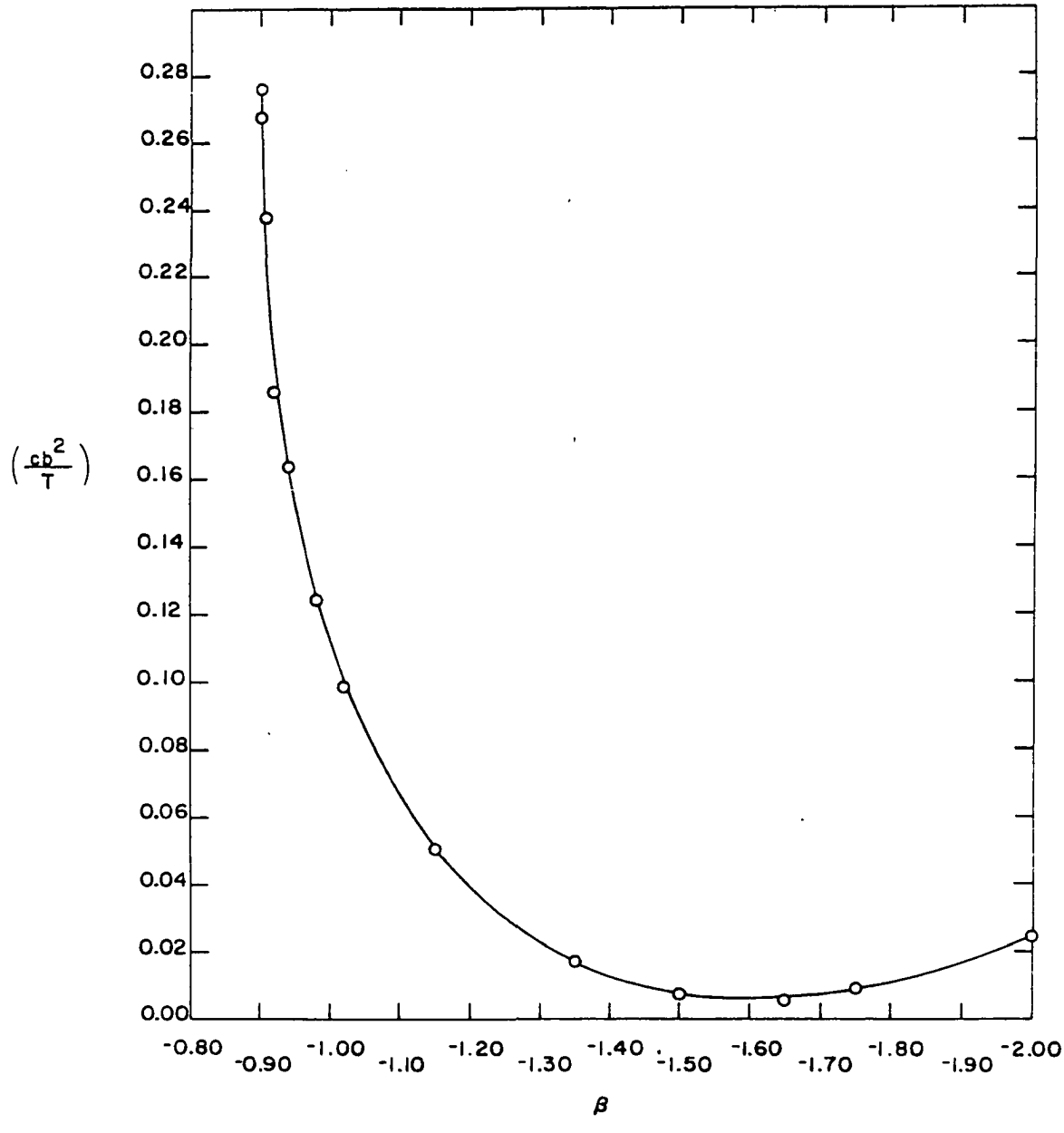

Figure 20. Change in value of the term containing the volume parameter during the first stage of separation

Separating Droplet - Second Stage

The model which was developed to include the additional resistance to separation of the surrounding fluid contains two parameters β and V. Since the velocity could not be adequately measured with the experimental equipment available, this model was tested by determining if any members of this two parameter family of curves were similar to those observed experimentally. This certainly is not a completely satisfactory test but it should give some indication, if the velocities needed to generate the profiles are reasonable.

If during this portion of the separation, the flow effects on the inside of the droplet were not negligible, their influence on the profile is probably of the same form and that observed is only the net result of the two flows.

Because of the approximate nature of this model, Equations 36-38 were not iterated to obtain an accurate value for $(\phi_i - \phi_{i-1})$. Instead, the magnitude of the change over the previous increment was used to evaluate the normal force due to the deflected stream. This force should be small in comparison to that of the normal stream and the error involved should be negligible.

Comparisons between experimental and computed profiles are given in Figures 21 and 22. The agreement at best indicates that the forces acting on the top of the droplet have been approximated. Due to the nature of the equation, some force of this nature must be acting if β is to decrease during the final stages of separation. What is needed is a good model for the flow outside of the droplet along with some means of estimating the

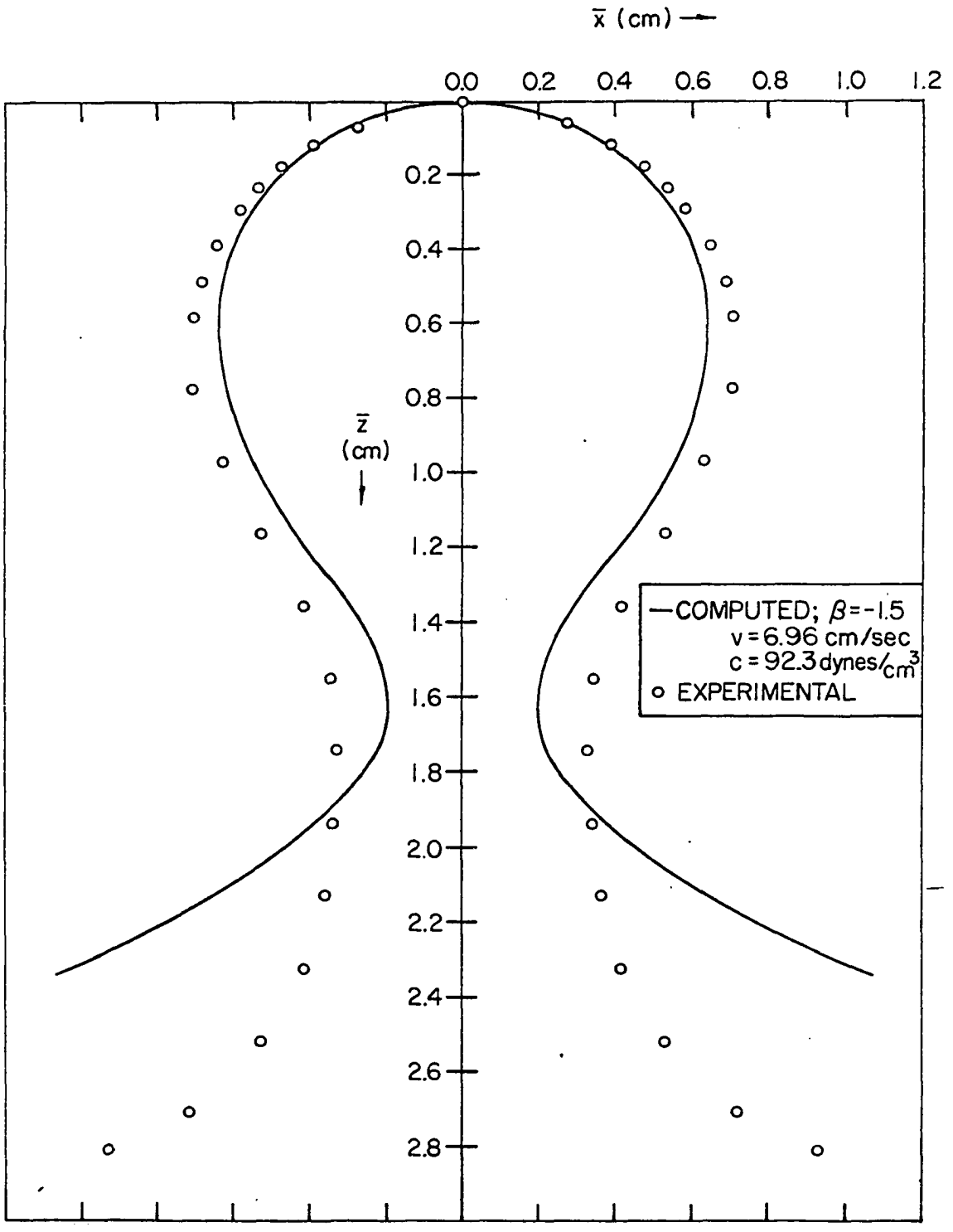

Figure 21. Profile of the separating droplet during the initial portion of the second stage of separation

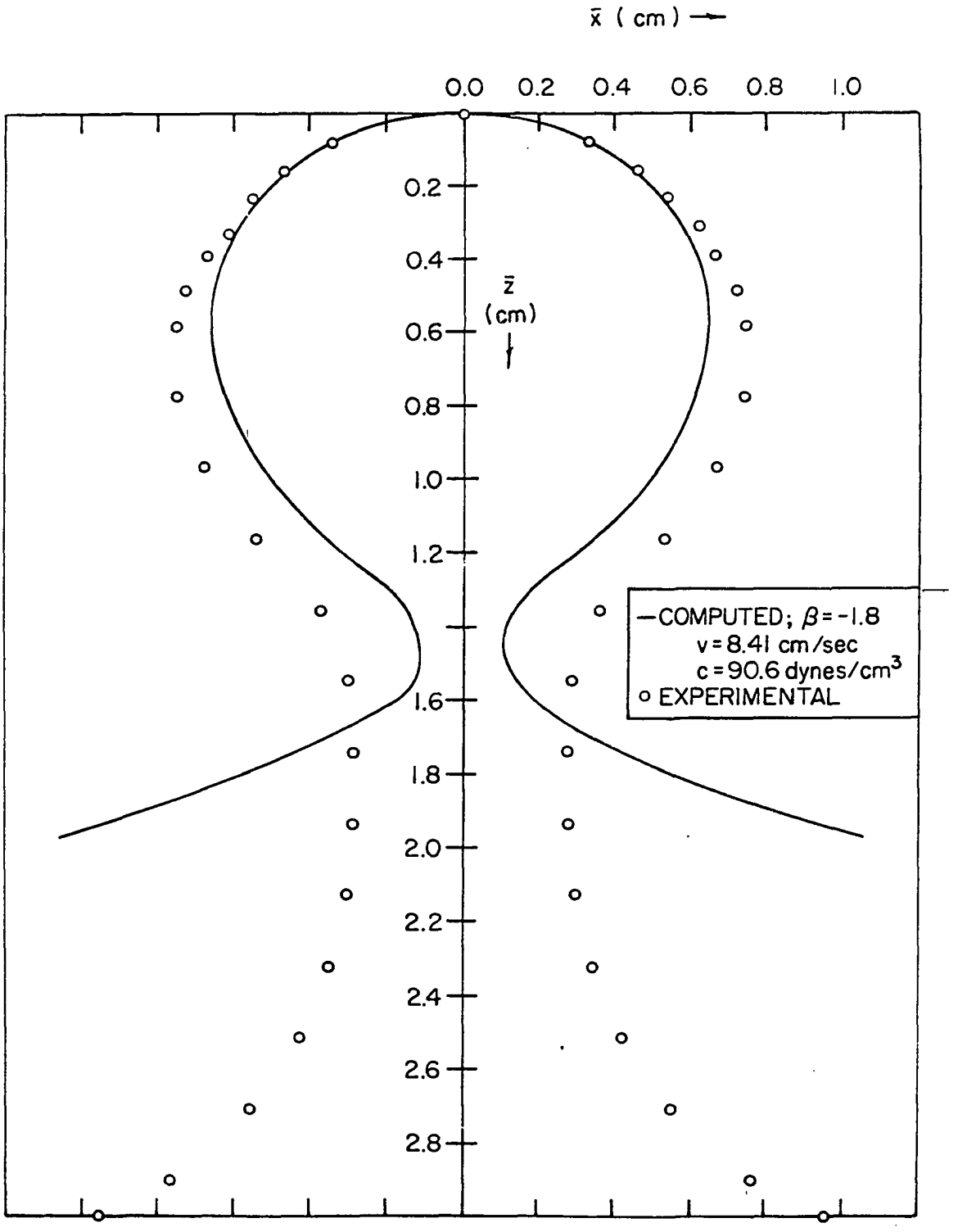

Figure 22. Profile of the separating droplet near the midpoint of the second stage of separation

resulting velocity distribution. The normal component of the velocity head could then be added to the force balance on each element of the interface.

CONCLUSIONS AND RECOMMENDATIONS

Conclusions

(1) The equations developed to describe the profile of a forming droplet provide a good representation of the actual profile over the range of conditions investigated for the Varsol-mineral oil-water system. Unfortunately, the equations apply only as long as the volume is less than the critical value.

(2) An estimate of the importance of the dynamic terms can be made prior to any integration by estimating f using the parameter β. When f is small relative to 2.0, the results for static droplets may be used to describe a forming droplet below the critical volume.

(3) The addition of the volume parameter c to the static equations resulted in profiles which compare favorably to those of a separating droplet during the first portion of the separation process for the system used.

(4) The resistance of the outside fluid appears to be the significant effect which must be added to the equations when a minimum develops in the profile.

Recommendations

(1) The models developed to apply to forming and separating droplets should be tested using different plate materials and fluid systems.

(2) Different flow models should be developed to account for the resistance of the surrounding fluid for a separating droplet which has a minimum in the profile.

(3) Additional work is needed to include the flow terms in the equations developed for the separating droplet in order to describe a forming droplet whose volume is greater than the critical value. One possible approach would be to use an energy balance over the droplet to determine which value of c should be used for a given volume. The value of c which gave the minimum energy for a given value of β and a known flow rate should produce the profile of the actual droplet.

(4) The equations developed for the forming and separating droplets have been tested only when the droplet rises upon separation. Although these equations should also apply to hanging droplets, this should be verified.

NOMENCLATURE

a - arc length

b - radius of curvature at the origin, cm.

c - constant, dynes/cm^3.

D - density of the droplet fluid, g/cm^3.

d - density of the external fluid, g/cm^3.

e - constant, dynes/cm^2.

F - normal force due to the impinging fluid, dynes

f - dimensionless group

g - gravational constant, 980cm/sec^2.

L - length

m - mass flow rate, g/sec.

P - pressure due to the internal fluid, dynes/cm^2.

p - pressure due to the external fluid, dynes/cm^2.

R - orifice radius, cm.

r - radius of curvature of the droplet

S - momentum rate, dynes

s - surface area, cm^2.

T - surface tension, dynes/cm.

V - velocity, cm/sec.

X - interface coordinate

Z - interface coordinate

β - dimensionless group

ϕ - normal angle, radians

ρ - radius of curvature of the droplet

θ - angle, radians

Subscripts

i - increment number

o - origin

r - orifice

Superscripts

_ - dimensioned variable, cm., (e.g. $\overline{X}$ = Xb)

BIBLIOGRAPHY

1. Laplace, P. S. Treatise on capillary action. Mechanique Celeste, Supplement to Book 10. 1806. Original not available; cited in Bashforth, F. and Adams, J. An attempt to test the theories of capillary action. P. 5. University Press, Cambridge, England. 1883.

2. Bashforth, F. and Adams, J. An attempt to test the theories of capillary action. University Press, Cambridge, England. 1883.

3. Lohnstein, T. Weiteres zur Theorie der fallenden Tropfen, nebst einen Ruckblick auf altere theoretische Versuche. Annalen der Physik 22:767-781. 1906.

4. Freud, B. and Harkins, W. The shapes of drops and the determination of surface tension. Journal of Physical Chemistry 33:1217-1234. 1929.

5. Poutanen, A. and Johnson, A. Studies of bubble formation and rise. Canadian Journal of Chemical Engineering 38:93-101. 1960.

6. Null, H. and Johnson, H. Drop formation in liquid-liquid systems from single nozzles. American Institute of Chemical Engineers Journal 4:273-281. 1958.

7. Hayworth, C. and Treybal, R. Drop formation in two-liquid-phase systems. Industrial and Engineering Chemistry 42:1174-1181. 1950.

8. Batson, J. Drop formation in liquid-liquid systems. Unpublished M.S. thesis. Library, University of Tennessee, Knoxville, Tennessee. 1951.

9. Harkins, W. and Brown, F. The determination of surface tension (free surface energy) and the weight of falling drops: the surface tension of water and benzene by the capillary height method. Journal of the American Chemical Society 41:499-524. 1919.

10. Rao, E., Kumar, R. and Kuloor, H. Drop formation studies in liquid-liquid systems. Chemical Engineering Science 21:867-880. 1966.

11. Nesis, E. Mechanism of detachment of bubbles from an unwettable horizontal plane. Academy of Sciences of the U.S.S.R. Proceedings 165:871-873. 1965.

12. Manfre, G. Rheological aspects of drop formation. Journal of Applied Physics 37:1955-1962. 1966.

13. Scriven, L. On the dynamics of phase growth. Chemical Engineering Science 10:1-13. 1959.

14. Beek, W. and Kramers, H. Mass transfer with a change in interfacial area. Chemical Engineering Science 16:909-921. 1962.

15. Popovich, A., Jervis, R. and Trass, D. Mass transfer during single drop formation. Chemical Engineering Science 19:357-365. 1964.

16. Streeter, V. L. Fluid mechanics. McGraw-Hill, New York, New York. 1962.

ACKNOWLEDGEMENTS

The author wishes to express his appreciation to Dr. L. E. Burkhart for his guidance and encouragement. Special thanks are due to Mr. Harvey Jensen for the countless number of times he assisted in the design and construction of the apparatus. Mr. Anthony Scott should be thanked for his assistance during most of the experimental runs. Finally, I would like to thank my wife for her endless patience and understanding during my graduate work.

APPENDIX

Derivation of the Equations of Bashforth and Adams

The first of the expressions can be derived by considering the geometry of a small segment of the profile of the droplet as shown in Figure 23.

$$\text{Cos}\theta = \frac{L+dX}{\rho} \tag{39}$$

$$\text{Cos}(\theta+d\phi) = \frac{L}{\rho} \tag{40}$$

Equations 39 and 40 may be combined:

$$\text{Cos}\theta = \text{Cos}(\theta+d\phi) + \frac{dX}{\rho} \quad . \tag{41}$$

This simplifies to:

$$\text{Cos}\phi d\phi = \frac{dX}{\rho} \, . \tag{42}$$

This expression may be combined with the arc length formula:

$$da = \rho d\phi \, , \tag{43}$$

to yield the required expression

$$\frac{dX}{da} = \text{Cos}\phi \quad . \tag{44}$$

Equations 43 and 44 are two of the equations used in the integration. The final equation can be derived using these two expressions. In the limit:

$$da^2 = dX^2 + dZ^2 \quad . \tag{45}$$

Equations 42 and 43 may now be substituted into this expression:

$$(\rho d\phi)^2 = (\rho \text{Cos}\phi d\phi)^2 + dZ^2 \quad . \tag{46}$$

Since dZ must always be positive:

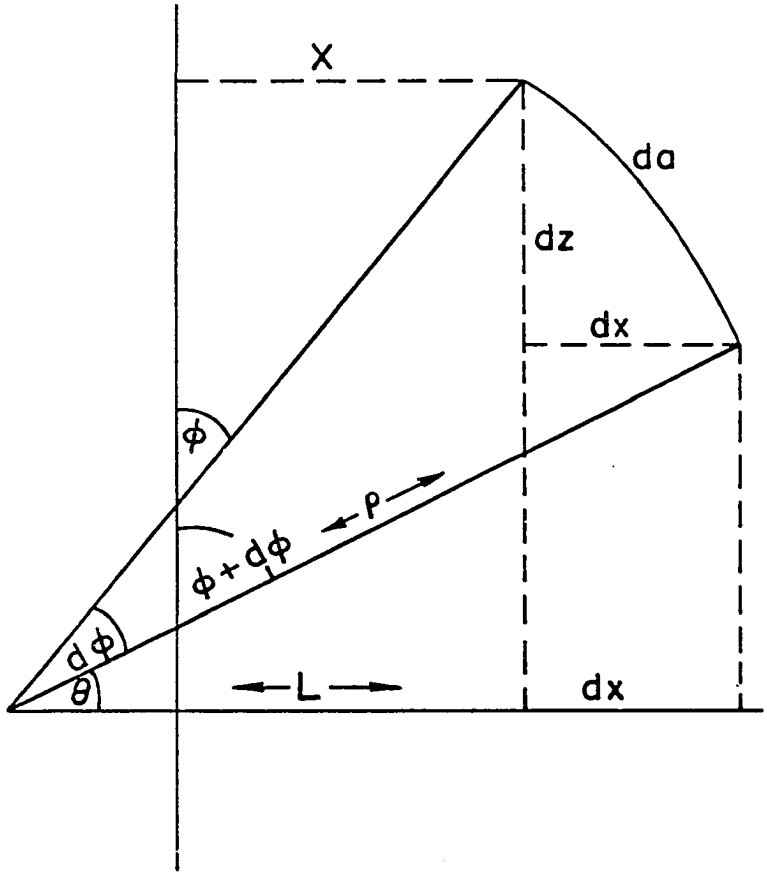

Figure 23. Geometry of the profile of the droplet

$$dZ = \rho \mathrm{Sin}\phi d\phi \quad . \tag{47}$$

In order to obtain the final relation this equation may be combined with the arc length formula to yield:

$$\frac{dZ}{da} = \mathrm{Sin}\phi \quad . \tag{48}$$

Derivation of the Equation of Laplace

Figure 24 is a section of the curved surface of the droplet. As the area of the section is increased, the change in area is:

$$dA = (d+dC)(B+dB) - CB \tag{49}$$

$$dA = BdC + CdB \tag{50}$$

The work done in increasing the area is:

$$W = T\ (BdC+CdB) \quad . \tag{51}$$

A pressure difference ΔP acts across the interface on the area BC through the distance dE. This resisting work to the increase in area is:

$$W = \Delta PBC\ (dE) \quad . \tag{52}$$

By comparing triangles in the figure:

$$\left(\frac{C+dC}{\rho+dE}\right) = \frac{C}{\rho} \qquad \text{or} \qquad dC = \frac{CdE}{\rho} \tag{53}$$

$$\left(\frac{B+dB}{r+dE}\right) = \frac{b}{r} \qquad \text{or} \qquad dB = \frac{BdE}{r} \quad . \tag{54}$$

When the forces are assumed to be balanced, the work tending to increase the interfacial area equals the opposing work due to pressure:

$$\Delta PBCdE = T\ (BdC + CdB) \tag{55}$$

This expression may be combined with the preceding equations to obtain the equation of Laplace:

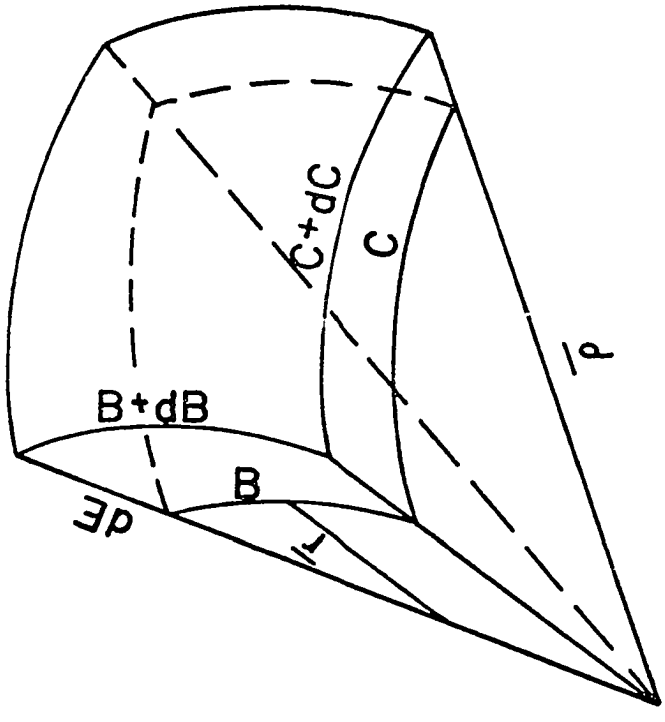

Figure 24. A section of the curved interface

$$\Delta p = T \left(\frac{1}{\rho} + \frac{1}{r}\right) \quad . \tag{56}$$

From Figure 23, the radius of curvature $\bar{r}$ is:

$$\bar{r} = \frac{\bar{X}}{\mathrm{Sin}\phi} \quad . \tag{57}$$

This may be substituted into Equation 48:

$$\Delta p = T \left(\frac{1}{\rho} + \frac{\mathrm{Sin}\phi}{\bar{X}}\right) \tag{58}$$